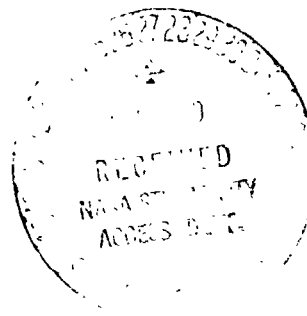# Compatibility of Elastomers in Alternate Jet Fuels

S. H. Kalfayan
R. F. Fedors
W. W. Reilly

June 1, 1979

ABSTRACT

The compatibility of elastomeric compositions of known resistance to aircraft fuels was tested for potential use in Jet A type fuels obtainable from alternate sources, such as coal. Since such fuels were not available at the time, synthetic alternate fuels were prepared by adding tetralin to a petroleum based Jet A type fuel to simulate coal derived fuels which are expected to contain higher amounts of aromatic and hydroaromatic hydrocarbons. The elastomeric compounds tested were based on butadiene-acrylonitrile rubber (NBR), a castable Thiokol polysulfide rubber (T), and a castable fluorosilicone rubber (FVMQ). Batches of various cross-link densities of these rubbers were made and their chemical stress relaxation behavior in fuel, air, and nitrogen, their swelling properties, and response to mechanical testing were determined. The object was to understand the nature of the chemical changes that take place in these elastomer compositions on aging and to be able to make approximate estimates of their service life from the data obtained.

PRECEDING PAGE ANK NOT FILMED

TABLE OF CONTENTS

Tables

Figures

SECTION I

INTRODUCTION

The purpose of this program was to investigate the effects of alternate jet fuels on polymeric materials used as fuel tank sealants and as parts that are exposed to jet fuels. Since there are differences in the chemical composition of petroleum-based jet fuels and jet fuels derived from coal and oil shale, it becomes necessary to determine the compatibility and aging effects of alternate fuels on polymeric compositions. Some expected differences in the fuels include increased percentage of aromatic and heterocyclic compounds and larger amounts of trace elements.

The experimental approach included chemical stress relaxation measurements on selected elastomeric compounds while they were in a fuel environment, sol-gel (extraction) determinations after aging in fuel, and stress-strain measurements at different strain rates and temperatures. From these measurements certain chemical changes in the polymers were determined, such as the nature and rate of degradation when the elastomer was stressed, the site of the breakdown, and the cross-link densities. The stress-strain measurements provided property surfaces which served as the basis for the prediction of the time to break in the absence of chemical degradation. Changes in the cross-link density, ν_e, after aging were used to estimate service life when chemical degradation was also present, as represented by change in ν_e.

Compounds made from three different elastomers were evaluated during the present task, namely, butadiene-acrylonitrile rubber (NBR), a Dow Corning fluorosilicone sealant (FVMQ), and polysulfide sealant PR 1422 (T). Castings or moldings with three different cross-link densities were made from NBR and FVMQ, and two from T. The stress relaxation of NBR and FVMQ compositions was measured in three fuels which differed in their aromatic hydrocarbon content. The fuels were supplied by NASA-Lewis Research Center and were described as follows:

1

Fuel I   - Jet A fuel (which originally contained about 20%
               aromatics, by volume.)

Fuel II - Jet A fuel + enough tetralin to yield 40% aroma-
               tics, by volume.

Fuel III - Jet A fuel + enough tetralin to yield 60% aroma-
               tics, by volume.

More extensive tests were made in Fuels I and III. The effects of Fuel
II were intermediate to Fuels I and III. Stress relaxation measurements
could not be carried out with T because it relaxes rapidly even at room
temperature. This is ascribed to disulfide-disulfide or sulfide-sulfide
interchange in the polysulfide network (Ref. 1).

SECTION II

EXPERIMENTAL

A.   PREPARATION OF VULCANIZATES

1.   Butadiene-Acrylonitrile Rubber (NBR)

Molded sheets of NBR were obtained from Parker Seal Company.
Three different batches, Nos. 1, 2 and 3, with increasing cross-link
densities, were supplied. No. 2 was the military specification material
N602-70. The sheets had been cured three minutes at 188°C (370°F) and
30 minutes at 107°C (225°F).

2.   Fluorosilicone Sealant DC 77-028 (FVMQ)

Three batches of vulcanizates, 1, 2 and 3, were prepared
using 4, 5 and 10 parts per hundred by weight, repsectively, of the
proprietary curing agent supplied by Dow-Corning with the base sealant,
DC 77-028, (FVMQ).

The preparation and cure of the sealant was carried out as
follows: the base sealant and the required amount of catalyst were

2

weighed within $\pm$ 0.01 g and then mixed by hand thoroughly for 8-10 minutes. The mixture was then degassed (<2 mm Hg) for $\frac{1}{2}$ to 1 hour depending upon the quantity of the mixture, which varied from 150 to 600g. Occasionally, the vacuum was broken to facilitate the degassing. Using an inert gas rather than air to break the vacuum seemed to enhance the efficiency of degassing. The mixture was then transferred into suitable molds, and sheets of two different thicknesses were cast: 1.78 mm (0.070") for tensile measurements, and 0.51 mm (0.02") for stress relaxation measurements. Any occluded air, along with excess sealant, could be pressed out into the perimeter of the casting to give bubble-free, flawless sheets. The sealant around the perimeter was discarded.

Cure was effected according to the following schedule:
48 hrs. at room temperature: 24 $\pm$ 2°C (75 $\pm$ 3°F)
24 hrs. at 71 $\pm$ 1°C (160 $\pm$ 2°F)
1 hr. at 149 $\pm$ 1°C (300 $\pm$ 2°F)
5 hrs. at 230 $\pm$ 2.2°C (448 $\pm$ 4°F) in dry nitrogen.

3.   Polysulfide Sealant PR 1422 (T)

The polysulfide sealant (T) was supplied premixed in frozen cartridges by Products Research and Chemical Co. of Burbank, CA. After thawing out, the material was cast in the same manner as the FVMQ. Only 1.78mm thick sheets were cast from which ring specimens were prepared for tensile testing. The castings were cured at room temperature for 48 hours and for 1 hour at 149°C (300°F). Two batches, T-1 and T-2, with increasing v_e, were prepared.

B.   STRESS RELAXATION MEASUREMENTS

1.   Description of the Relaxometer

The relaxometer used for the measurement of stress decay, shown in Figure 1, consists of a low-force-range load cell placed outside the oven, test specimens and grips housed in the gas-tight cylindrical test chamber mounted in the oven, and a movable cylinder attached
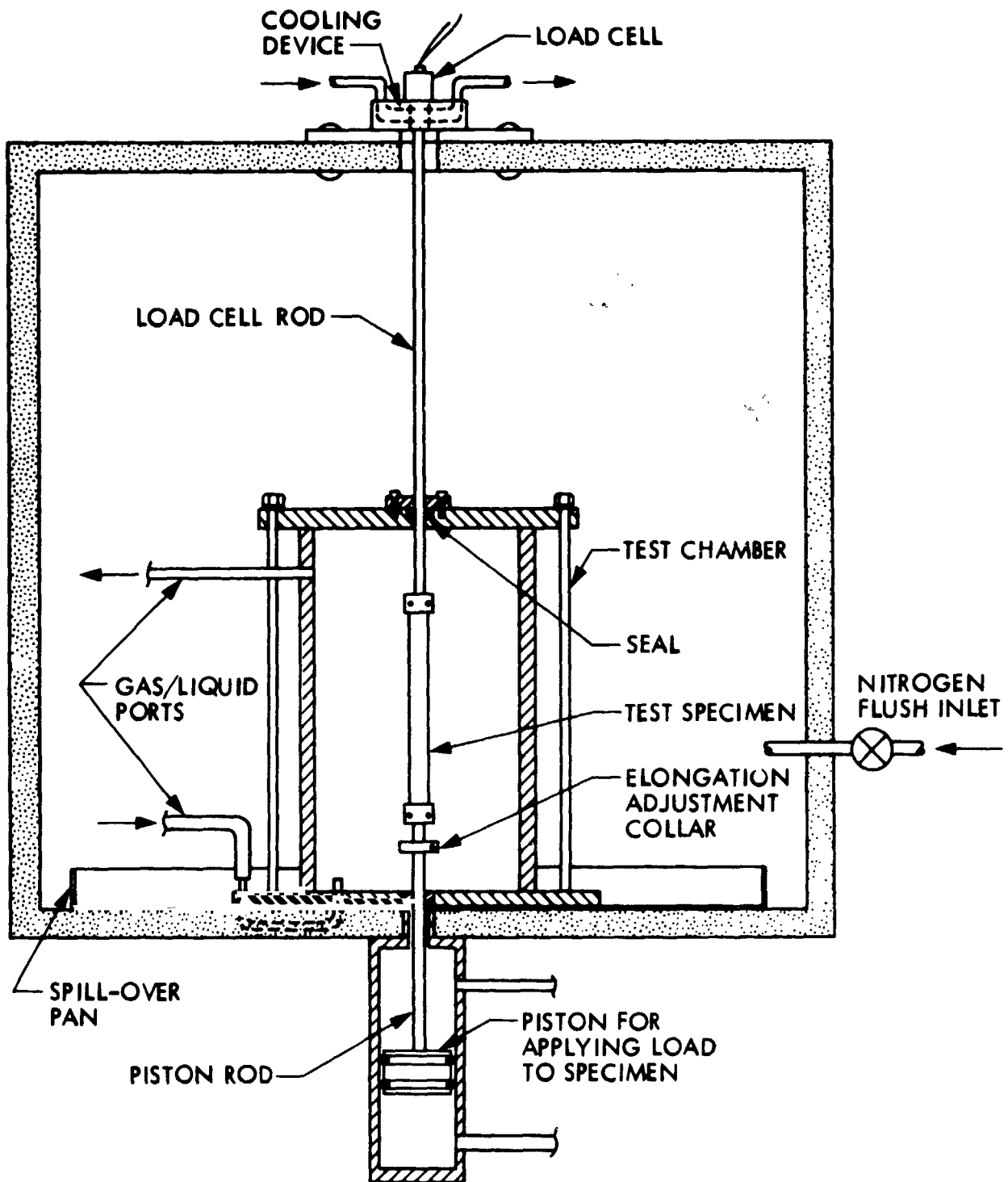
Figure 1. Schematic of High Temperature Gas and Liquid Stress Relaxometer

to the lower grip which provides the desired elongation of the rubber specimen. The upper grip is attached to the load cell, which measures the force. The load cell is maintainted at or near room temperature by the continuous circulation of water in a heat exchanger. The temperature in the test chamber and the oven and the electrical output of the load cell are monitored remotely.

2.   Measurements in Nitrogen, Fuel and Air

For measurements in any fluid environment, dogbone specimens 12.70 mm wide, 68.58 mm long and approximately 0.50 mm thick were used at 28.5% extension. For measurements in nitrogen, the chamber was first flushed several times with pure nitrogen, and thereafter a steady flow of the inert gas was maintained during the entire course of the test. For measurements in alternate fuels, the chamber was filled with the liquid from a reservoir connected to the chamber. The oven was flushed with nitrogen to minimize fire hazards. There were no precautions required for measurements made in air. For intermittent stress relaxation measurements, the elastomer specimen was stretched for ten minutes and relaxed for fifty minutes.

C.   SWELLING MEASUREMENTS

Swelling measurements were made on NBR batch 1, FVMQ batch 3, and T-1 and T-2. Weighed samples of these elastomer compositions were immersed in large excess of n-butyl acetate at room temperature. After seven days, the swollen samples were removed, surface dried and weighed. The solvent was then driven off and the samples weighed again. Values of 0.8824, 1.2770, 1.3685 and 1.452 were used as densities of the solvent and of NBR 2, FVMQ 3, and T-1 and T-2, respectively.

D.   MECHANICAL TESTING

1.   Preparation of Ring Specimens

The stress-strain tests were carried out using ring specimens approximately 2.15 cm (0.85") inside diameter and 2.54 cm (1.0")

5

outside diameter. The rings were cut from vulcanized sheets using a high-speed rotary cutter mounted in a precision drilling machine. The spindle was operated at between 300 and 700 RPM, depending on the modulus of the sample, using distilled water as a lubricant to facilitate cutting. During the cutting operation, the sheet was adhered to a block of polyethylene using tape with adhesive on both sides (double-stick tape). After the sheet had been cut, the rings were carefully removed from the tape and the condition of the rings, especially the cut surfaces, were examined using a low-power magnifier.

2.   Stress-Strain Measurements

The uniaxial stress-strain response was measured using two Instron testing machines. One testing machine was used for the high temperature runs, i.e., test temperatures greater than 353 K (80°C) while the other machine was used for low temperature runs, i.e., est temperatures lower than 353 K (80°C). Test speeds were varied from 0.0508 cm/min (0.02in/min) to 50.8 cm/min (20in/min). The rings were placed on two 0.635 cm diameter (0.250 in) hooks mounted on the load cell and the movable crosshead, respectively. The stress was calculated using the following equation:

$$\sigma = \frac{f}{a(D_0 - D_i)} \qquad (1)$$

where f is the load, a is the thickness, and D_0 and D_i are the outside and inside diameter, respectively. The strain was calculated using

$$\varepsilon = \frac{2\ell}{\pi D_i} \frac{XS}{CS} \qquad (2)$$

where ℓ is the distance along the time axis of the Instron trace, XS is the crosshead speed and CS is the chart speed. In practice, the initial portion of the Instron trace is characterized by the occurrence of a "toe" which is produced during the time the initially circular specimen is strained sufficiently so that the specimen becomes parallel sided. The linear portion of the trace corresponding to the stretching of the parallel sided specimen was extrapolated to zero load and this point was taken as the zero of the time scale as well. The time was calculated using $t = \varepsilon/R$ where R is the strain rate defined by $R = 2XS/\pi D_i$. Nor-

6

mally, about 10-20 points, including the break point, were read from the Instron chart and converted to σ and ε values.

3.   Swollen Stress-Strain Measurements

Some stress-strain measurements were made on the swollen 'scomers for the determinations of cross-link densities. The apparatus use is shown in Figure 2. Weighed specimens 12.70 by 76.2 mm and about 0.5 mm thick were immersed in n-butyl acetate until equilibrium was established, which took 6-7 days. The swollen samples were surface dried and weighed. They were then placed singly in the swollen-stress-strain tester. After inserting two pins vertically apart by 37 mm, the sample was stressed by adding loads to the beam balance and the strain, i.e., the change in the distance between the two pins was measured with a cathetometer. The swollen samples were then dried and weighed.

E.   AGING EXPERIMENTS

Weighed ring specimens of each of the three rubbers were placed in sealed, stainless steel pressure tubes, filled with the various fuels and heated at different temperatures. Each ring could be identified by its position on a hanger that was placed in each tube. Samples were withdrawn periodically and their cross-link densities were calculated from the swelling and stress-strain measurements performed.

SECTION III

RESULTS AND DISCUSSION

A.   CHEMICAL STRESS RELAXATION MEASUREMENTS

Developed by A. Tobolsky and others (Ref. 2), this method has a unique value for the study of changes in the network of polymers during aging. Information, such as degradation rates, the nature of degradation, i.e., bond scission, cross-linking, or both, the site of scission, whether at the backbone chain or at the cross-link, can be
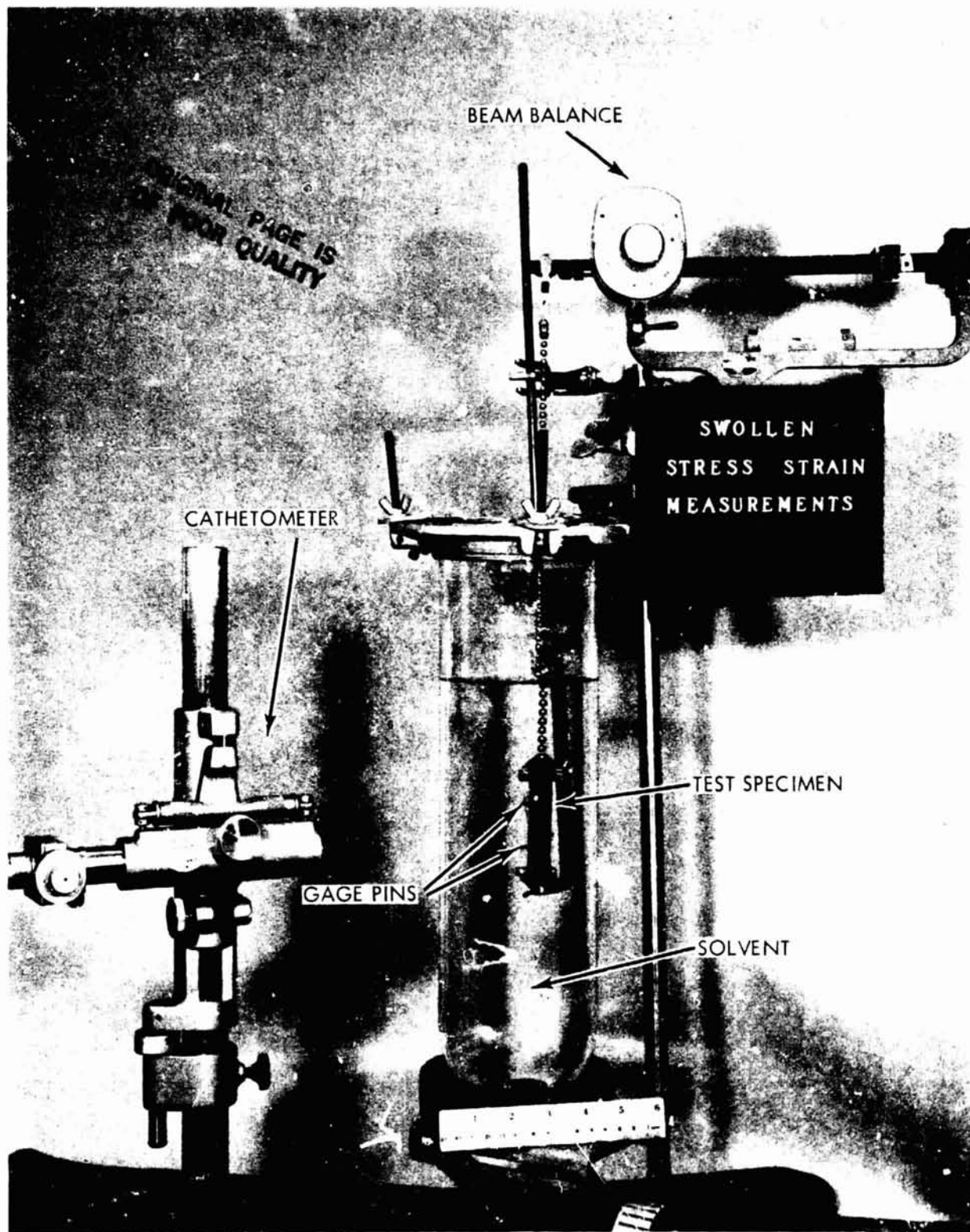
7

Figure 2. Apparatus for Measuring Swollen Stress-Strain of Elastomers

obtained from chemical stress relaxation measurements. Two types of chemical stress relaxation measurements can be made: a) continuous, in which the sample is held at constant strain (extension) throughout the experiment; and b) intermittent, in which the sample is strained only at such times as the stress is measured. According to network theory, the decrease in stress in a continuously-stretched sample is a direct measure of the number of network chains broken. It is assumed that new networks formed, while the elastomer is strained, will not contribute to stress when the sample is strained, as is the case in the intermittent type of stress relaxation. The intermittent measurements show the stress due to the residue of the original network plus the stress due to the new network, and may differ considerably from the continuous measurements. If only scission were occurring, the continuous and intermittent curves, obtained by monitoring the stress relaxation, would be identical. If, on the other hand, the stress at a given time in the intermittent experiment is larger than that in the continuous experiments, the difference would represent the contribution to the network of any new cross-links formed during aging (Ref. 3).

1.   Stress Relaxation of NBR in Fuels I, II and III

Three different batches of NBR, 1, 2 and 3, were tested in the three fuels. The cross-link densities were obtained from both stress-strain and swelling measurements. Values obtained from swelling measurements were lower than those resulting from stress-strain measurements. The cross-link density range from either source was, however, large enough to assess clearly the influence of aging on cross-link density and vice-versa. The v_e values obtained from swelling measurements are given in Table 1.

NBR 2, commercial designation N 602-70, is the military specification material and has an intermediate $v_{e(o)}$. Figure 3 shows the chemical stress relaxation of this rubber in the three fuels at various temperatures. It can be seen that its reduced stress, f_t/f_o, where f_t and f_o are tensile forces at time t and t_o, decays to zero in a matter of minutes at 120°C in Fuel III. The relaxation is slower in Fuel I and has an intermediate rate in Fuel II. As expected, the rate

9

TABLE 1. CROSS-LINK DENSITIES

Batch	UNAGED $\nu_{e(o)}$ moles/m³	AGED				
		Medium	Aging Temp. °C	Duration h	$\nu_{e(t)}$ moles/m³	% Change in ν_e
T-1	90.0	Fuel I	150	160	22.5	- 75
			140	160	42.7	- 52.5
		Fuel III	150	160	15.7	- 82.5
			140	160	29.0	- 68.0
T-2	278.0	Fuel I	80	160	281	+ 1.1
			100	160	283	+ 1.8
			120	120	289	+ 4.0
		Fuel III	80	160	298	+ 7.2
			100	160	296	+ 6.5
			120	120	288	+ 3.6
NBR-1	73.0					
NBR-2	260.0	Fuel I	140	160	570	+119.2
			150	160	321	+ 23.5
		Fuel III	140	160	218	- 16.1
			150	160	59.0	- 77.3
NBR-3	804.0					
FVMQ 1	8.1					
FVMQ 2	76.1					
FVMQ 3						
Casting a	240	Fuel I	150	240	161	- 33
	240	Fuel III	150	240	137	- 42
b	200	Fuel I	230	200	100	- 50
			230	1000	8	- 96
			250	200	43	- 73
			270	54	70	- 54
		*Fuel I vapor	227	2500	199	0

*Includes 300h exposure to liquid Fuel I at 60°C.
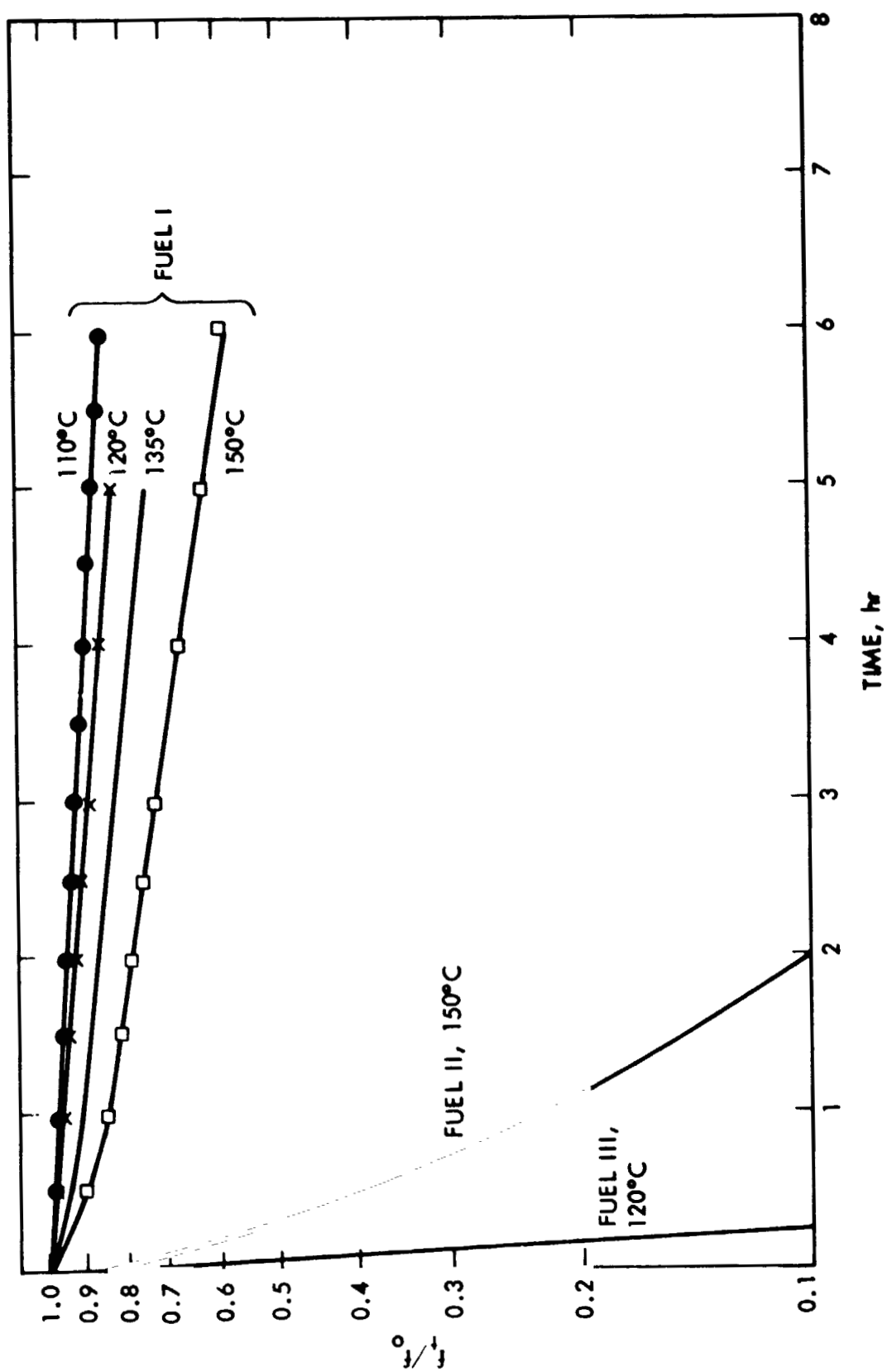
Figure 3. Stress Relaxation of NBR 2, in Fuels I, II and III at Various Temperatures

FUEL I

110°C
120°C
135°C
150°C

FUEL II, 150°C

FUEL III, 120°C

TIME, hr

f_t/f_0

1.0
0.9
0.8
0.7
0.6
0.5
0.4
0.3
0.2
0.1

1   2   3   4   5   6   7   8

11

of relaxation increases with temperature and seems to follow first order kinetics.

Figure 4 illustrates the effect of cross-link density on the stress relaxation of NBR in Fuels I and II at 150°C. It can be noticed that the stress relaxation of NBR is inversely proportional to the cross-link density, namely the higher the ν_e the lower the relaxation rate in any of the fuels. It has been shown that random scission along the polymer chain is indicated when the rate of relaxation is found to be inversely proportional to the cross-link density, and scission in the cross-link is indicated when the rate of relaxation is independent of the cross-link density (Ref. 3). The slower stress relaxation rate, shown by the higher cross-linked NBR, suggests that degradation occurs predominantly in the polymer chain, rather than at the cross-link.

The relaxation of NBR 1 and 2 in Fuel III at 120°C or above was so fast that meaningful data could not be obtained. Experiments in this fuel were, therefore, carried out with NBR 3. The influence of the highly aromatic fuels on the stress decay of NBR is also shown in Figure 5. When measured at 150°C, NBR relaxes approximately six times faster in Fuel III than in Fuel I. The influence of temperature on the relaxation rate of NBR 3 in Fuel III is shown in Figure 6. These and similar curves were used to calculate activation energies and for extrapolation to service life.

The extents of cross-linking that may occur simultaneously with scission during aging can be obtained by comparison of intermittent with continuous stress relaxation measurements. For intermittent measurements, the rubber is stressed for a short period and relaxed for a longer period, repeatedly. Figure 7 shows that cross-linking as well as scission takes place when NBR ages in Fuel III at 150°C. The number of additional cross-links, ν_e, is not very large as deduced from the closeness of the two curves and the results of computations made, which are shown graphically in Figure 8. For NBR 3, the number of additional network chains (cross-links) formed in 4 hours at 150°C amounts to about 7 moles/m^3 (see Figure 8, curve 3). The following equations were used to calculate the additional cross-links:

12
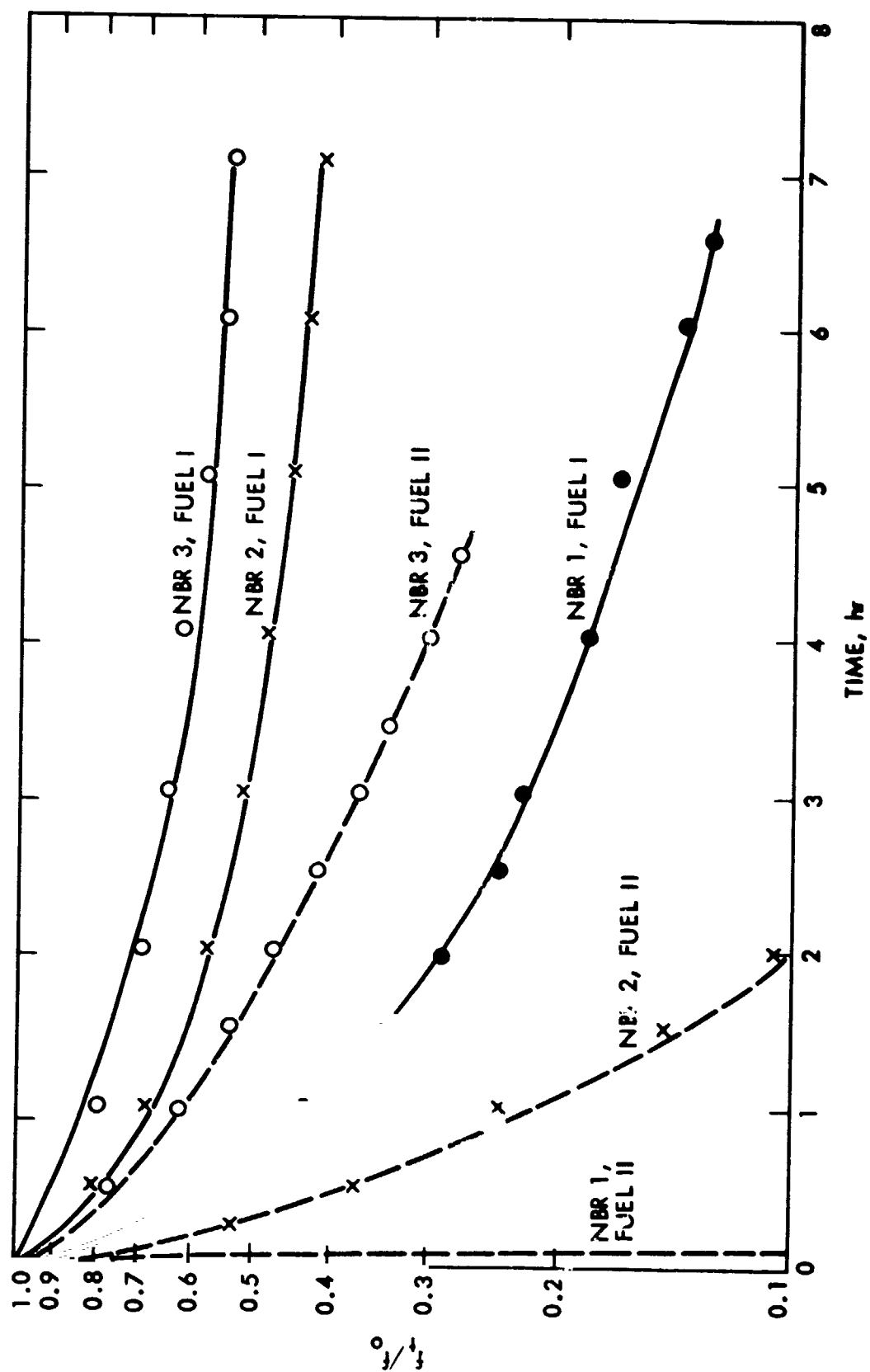
Figure 4. Continuous Stress Relaxation of NBR or Various ν_e, in Fuels I and II at 150°C

13

Figure 5. Stress Relaxation of NBR 3, at 150°C in Various Fuels
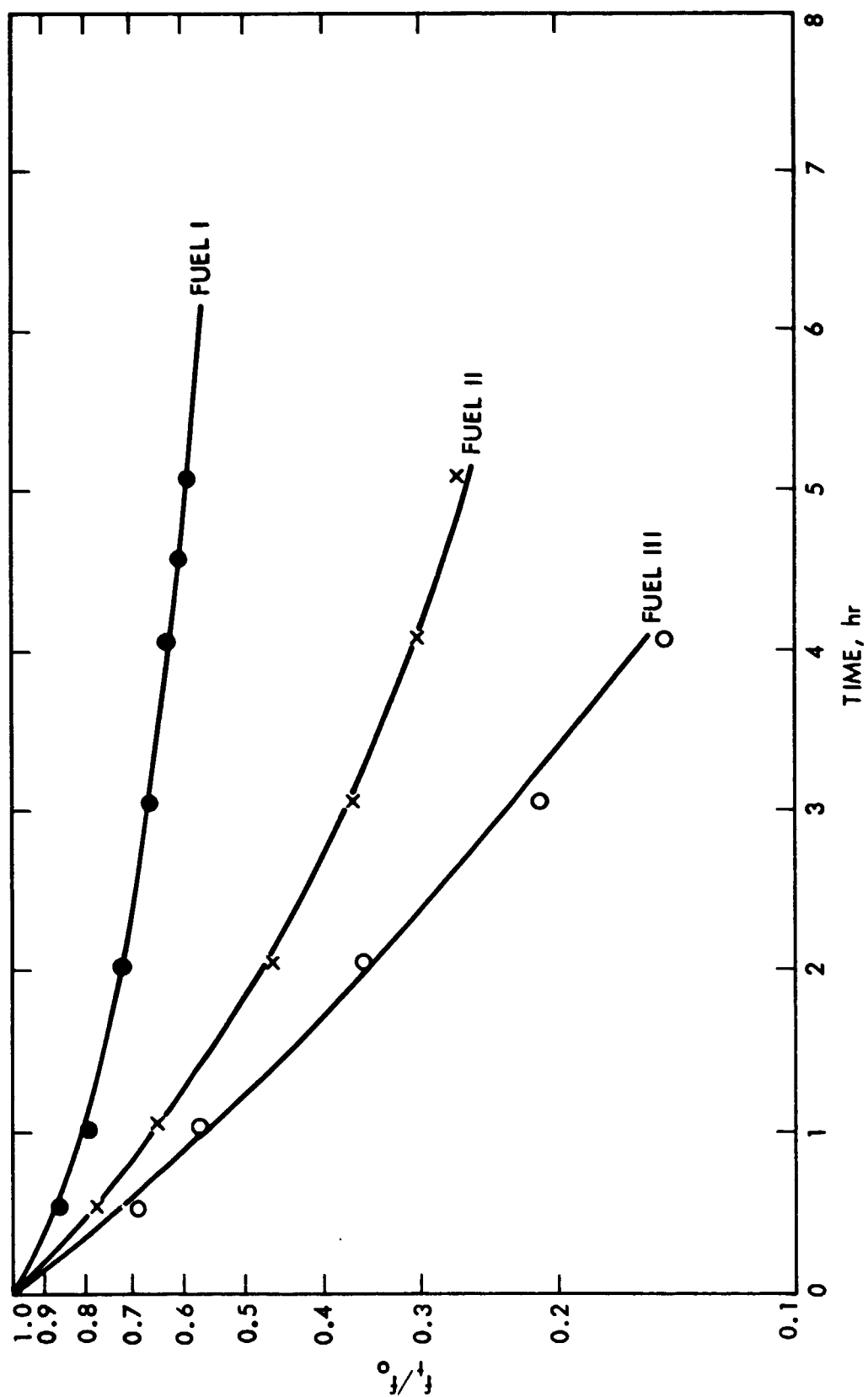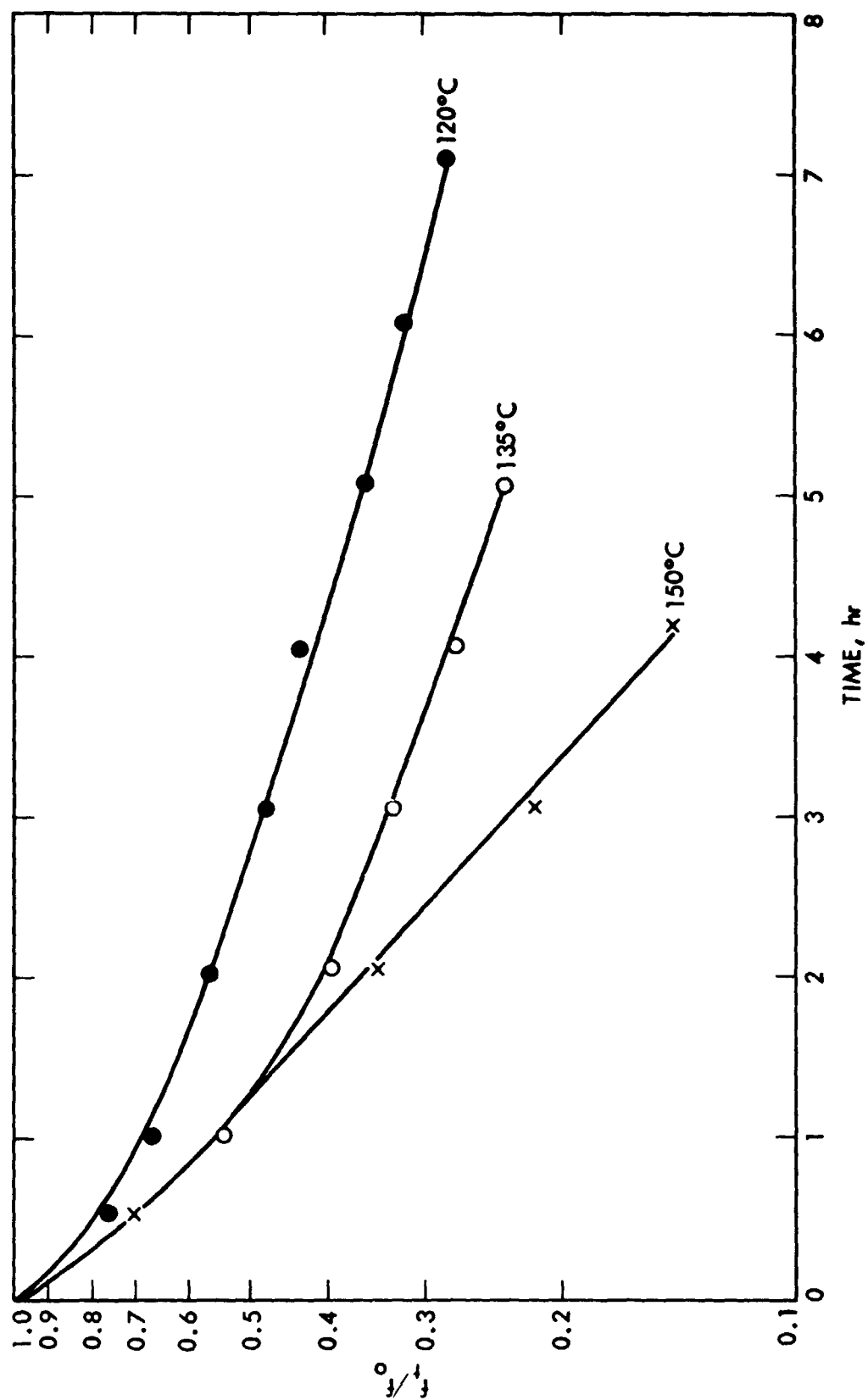
Figure 6. Stress Relaxation of NBR 3, in Fuel III at Various Temperatures
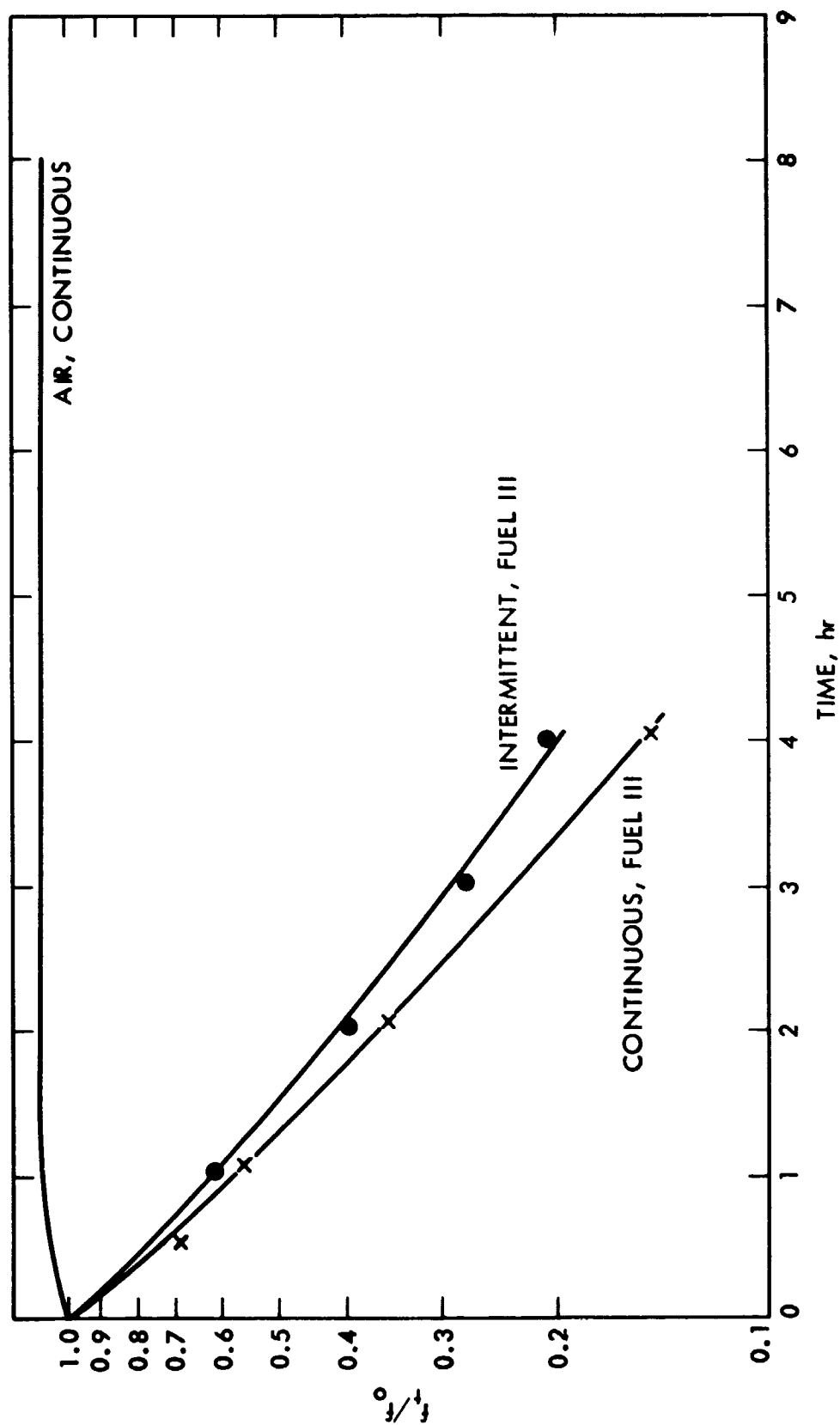
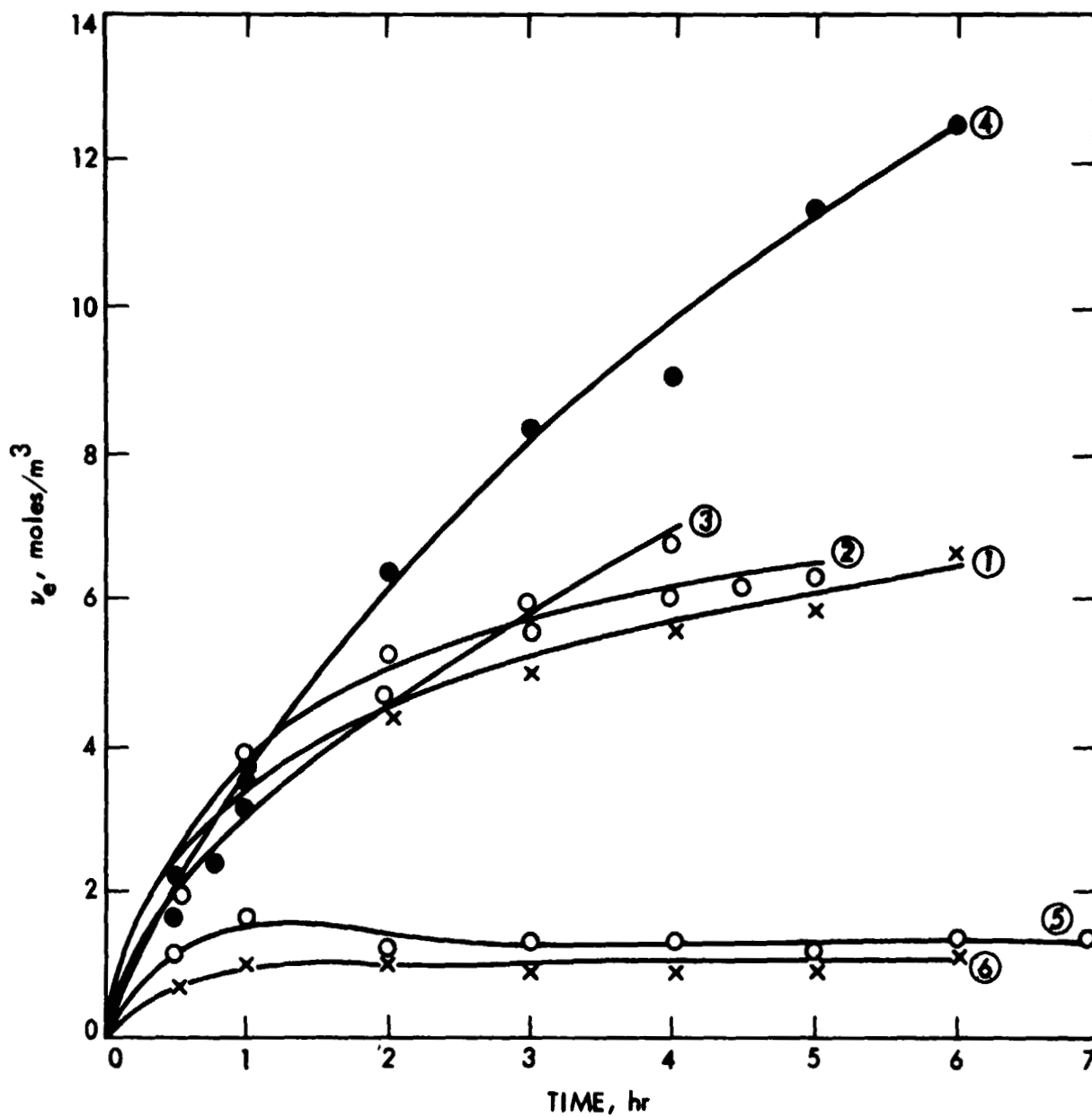Figure 7. Stress Relaxation of NBR 3, at 150°C in Fuel III and Air

Figure 8. Additional Network Chains Formed in NBR and FVMQ Based
Sealant Samples at 150°C. ① NBR 3 in Fuel I; ② NBR 3 in Fuel II;
③ NBR 3 in Fuel III; ④ NBR 2 in Air; ⑤ FVMQ 2 in Fuel I;
⑥ FVMQ 2 in Fuel III

$$\nu_{e(t)}/\nu_{e(o)} = (f_t^i - f_t^c)/f_o \qquad (3)$$

$\nu_{e(o)}$ was calculated from

$$\nu_{e(o)} = f_o/ART \left(\lambda - \frac{1}{\lambda^2}\right) \qquad (4)$$

where f_o = stress at time "zero," f_t = stress at time t (the super-
scripts i and c stand for intermittent and continuous); A = cross sec-
tional area of the sample, λ = extension ratio, and R and T have their
usual meanings. The terms $\nu_{e(t)}$ and $\nu_{e(o)}$ denote cross-link densities at
time t and "zero."

2.   <u>Stress Relaxation of FVMQ in Fuels I, II and III</u>

          The influence of temperature on the stress relaxation of
different FVMQ batches in Fuels I to III is shown in Figures 9 to 15.
Table 1 shows the unequal cross-link densities, $\nu_{e(o)}$, of the three FVMQ
batches. The changes in the stress relaxation with temperature are not
pronounced in the temperature range used (120-150°C for FVMQ 1, Figure
9, and 150-190°C for FVMQ 3, Figure 10). These temperatures are consi-
dered relatively low for this high temperature and hydrocarbon fuel-
resistant sealant.

          The relative effect of the three fuels on FVMQ 2 is shown in
Figure 11 and that of Fuels I and III on FVMQ 3 at 190°C is shown in
Figure 12. Although the stress relaxation rate of the sealants is higher
in Fuel III, the effect is not as pronounced as in the case of NBR.
Similar results, not shown, were obtained for FVMQ 1. This indicates
that the fluorosilicone sealant has relatively good aging properties in
highly aromatic fuels.

          The stress relaxation of FVMQ in Fuel III could not be
measured at temperatures higher than 190°C, because the rapid evapo-
ration of the tetralin constituent changed the nature of the remaining
fuel. Measurements at higher temperatures could be made in Fuel I, and
results given in Figures 13, 14 and 15 show the good resistance of FVMQ
1, 2 and 3 to hydrocarbon fuels.

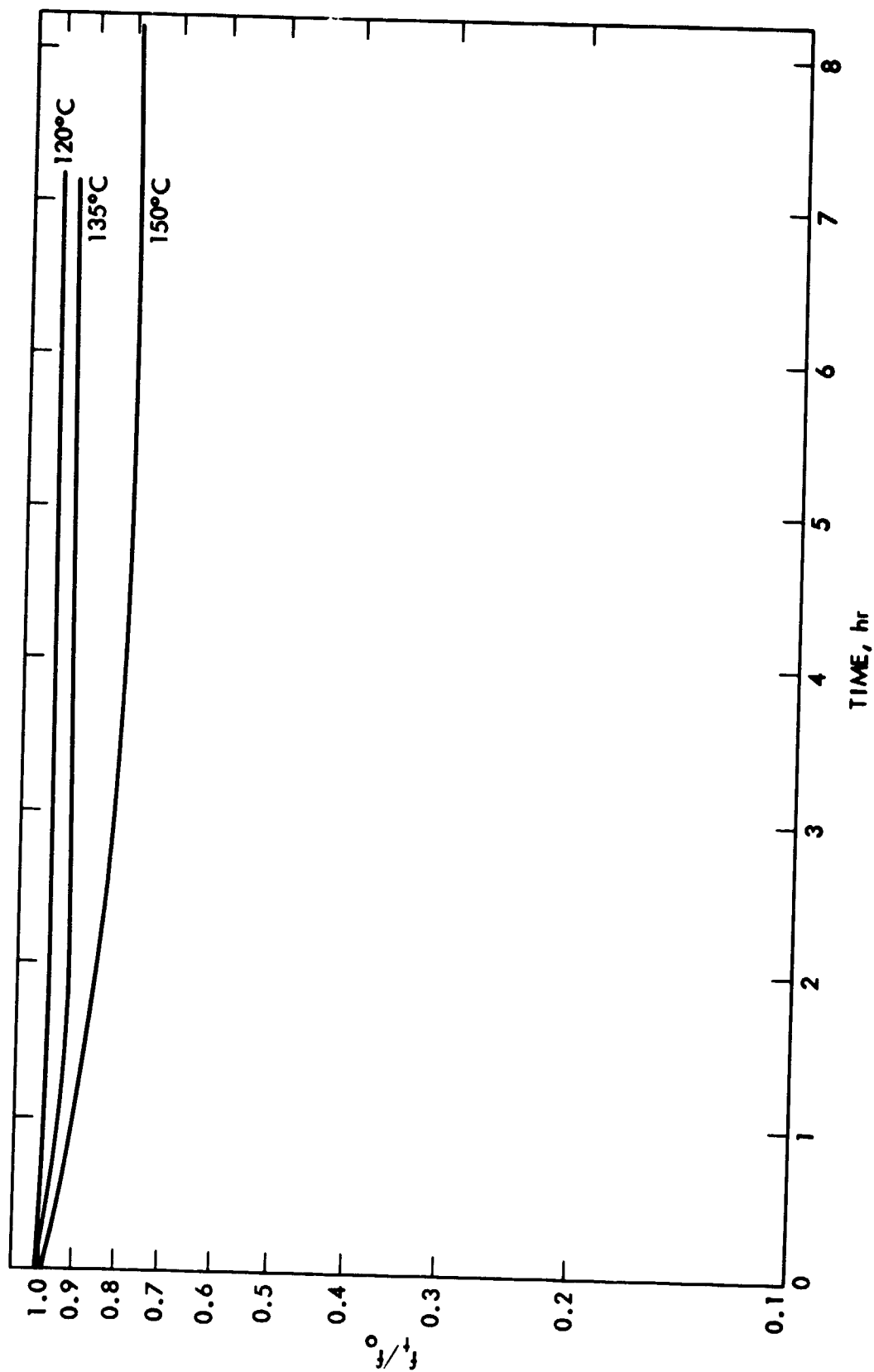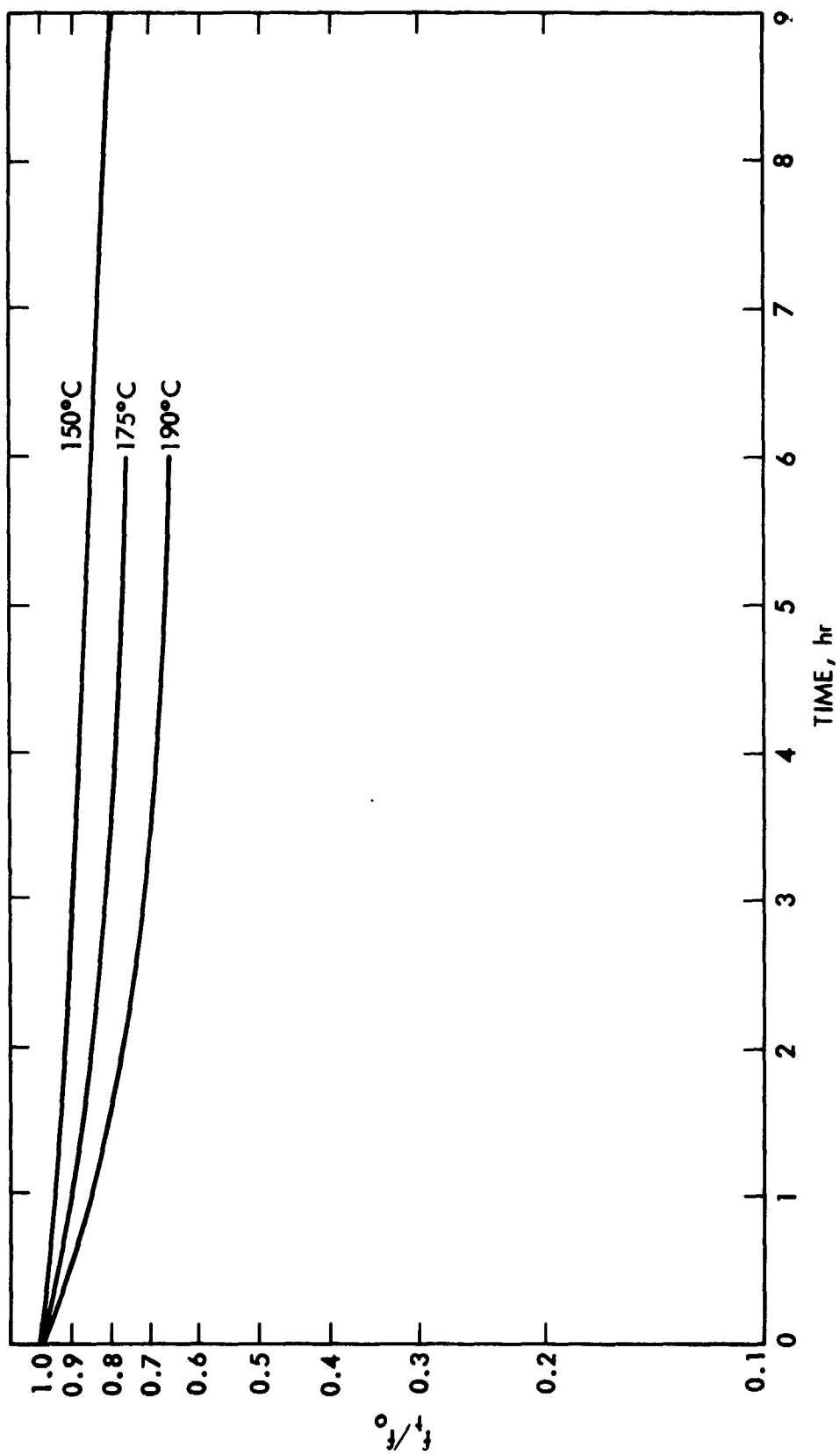Figure 9. Continuous Stress Relaxation of FVMQ 1 in Fuel III

19

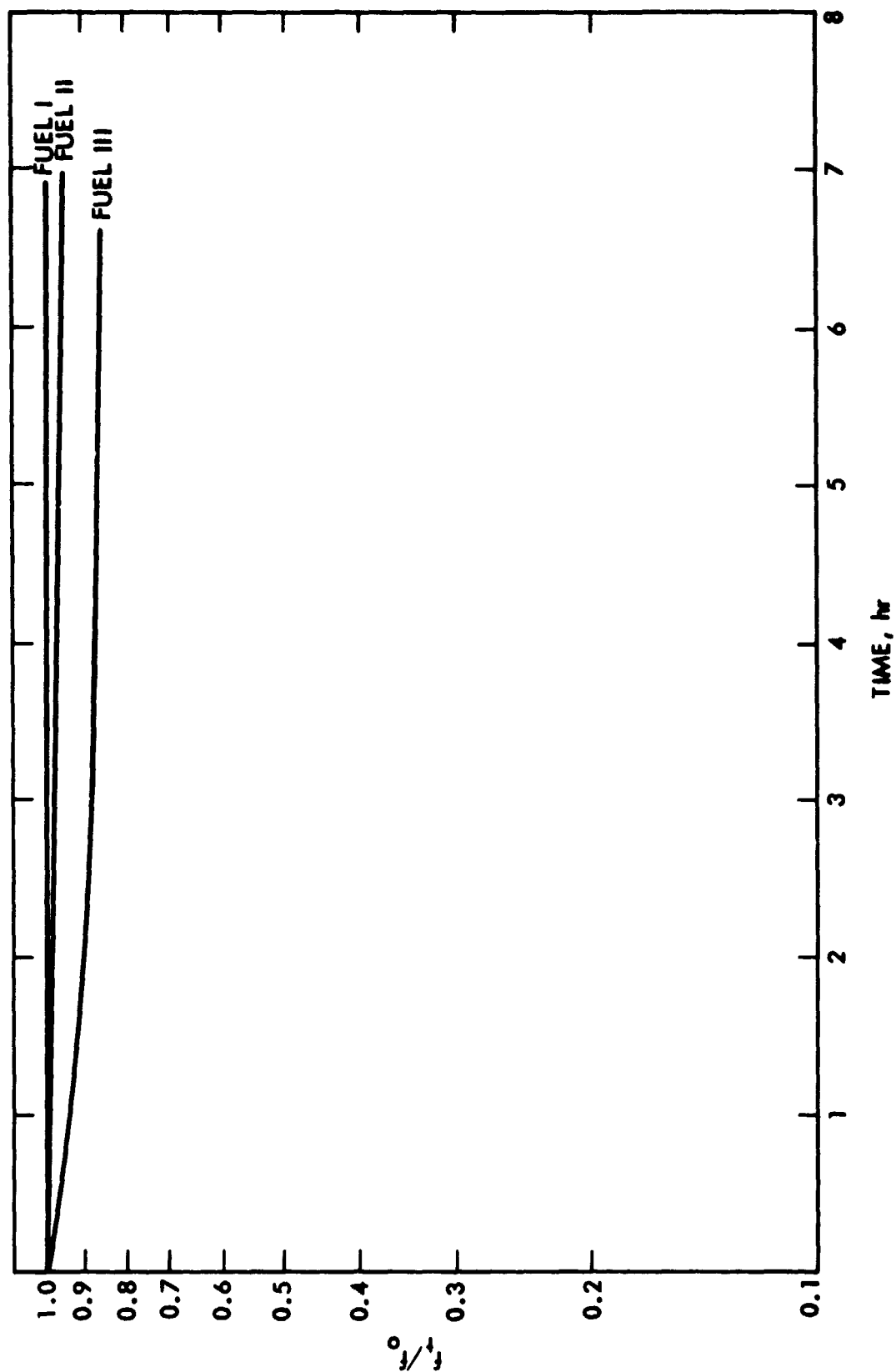Figure 10. Stress Relaxation of FVMQ 3 in Fuel III

Figure 11. Continuous Stress Relaxation of FVMQ 2 at 150°C in Various Fuels
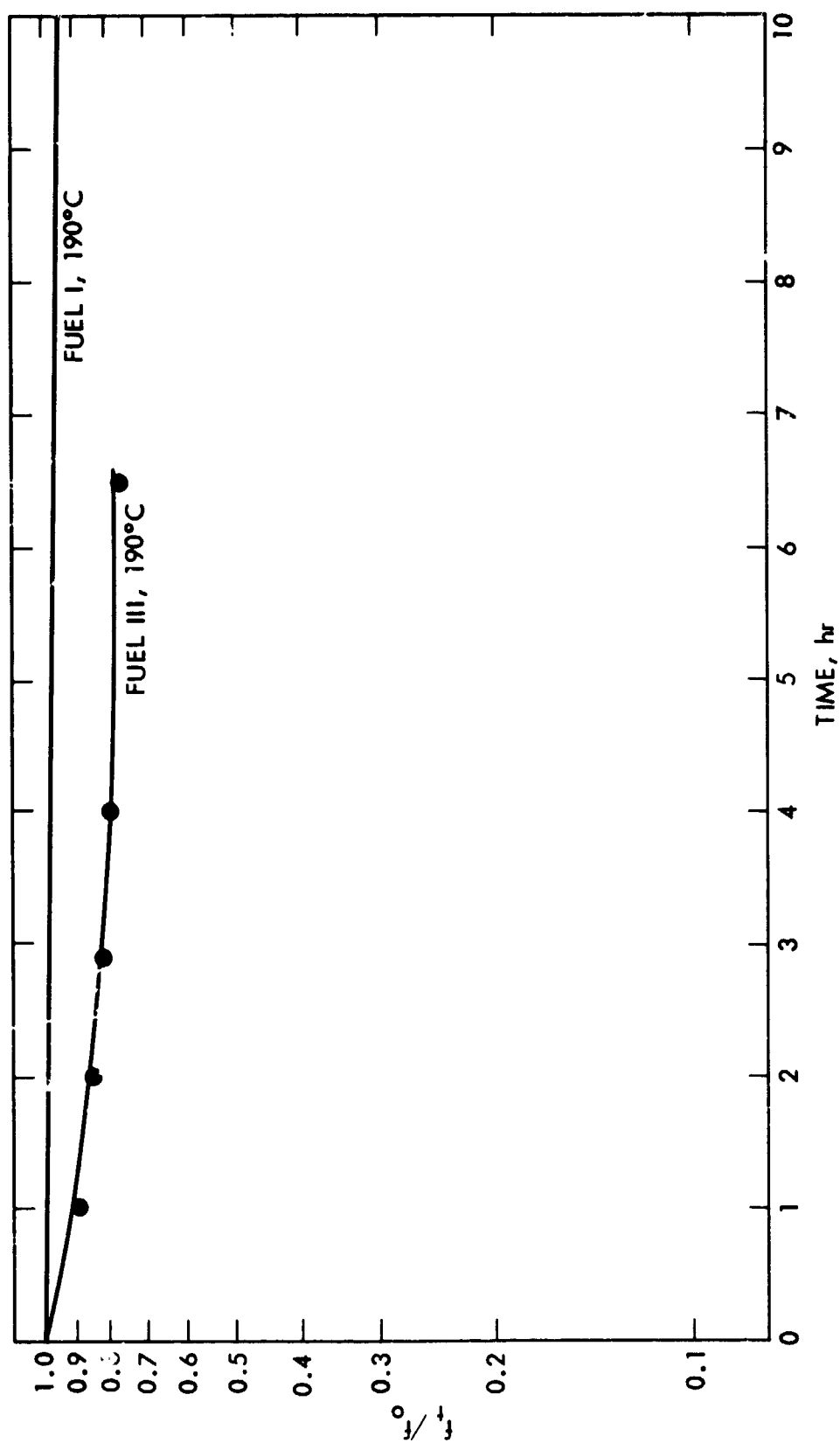
21

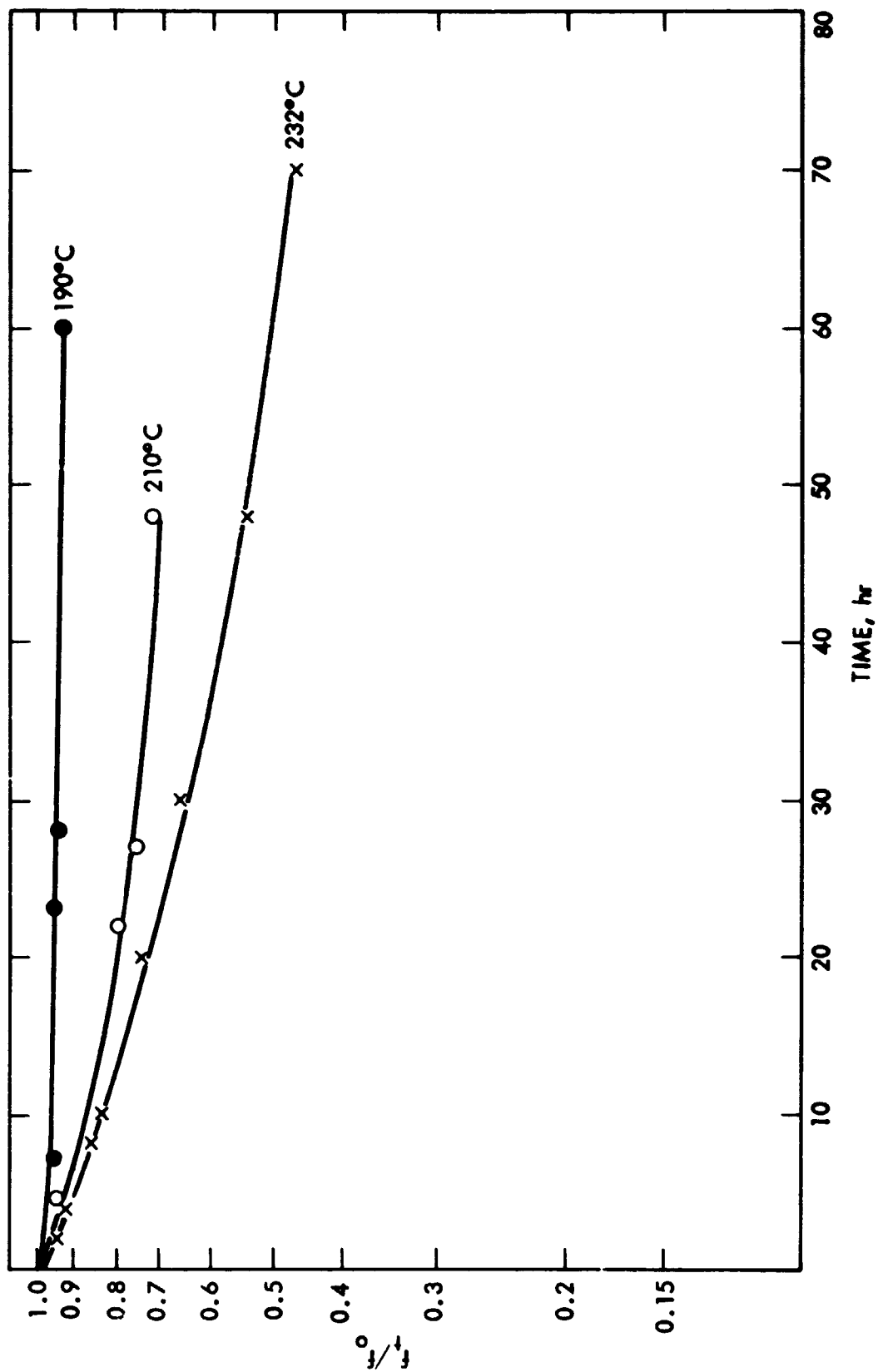Figure 12. Stress Relaxation of FVMQ 3 in Fuels I and III at 190°C

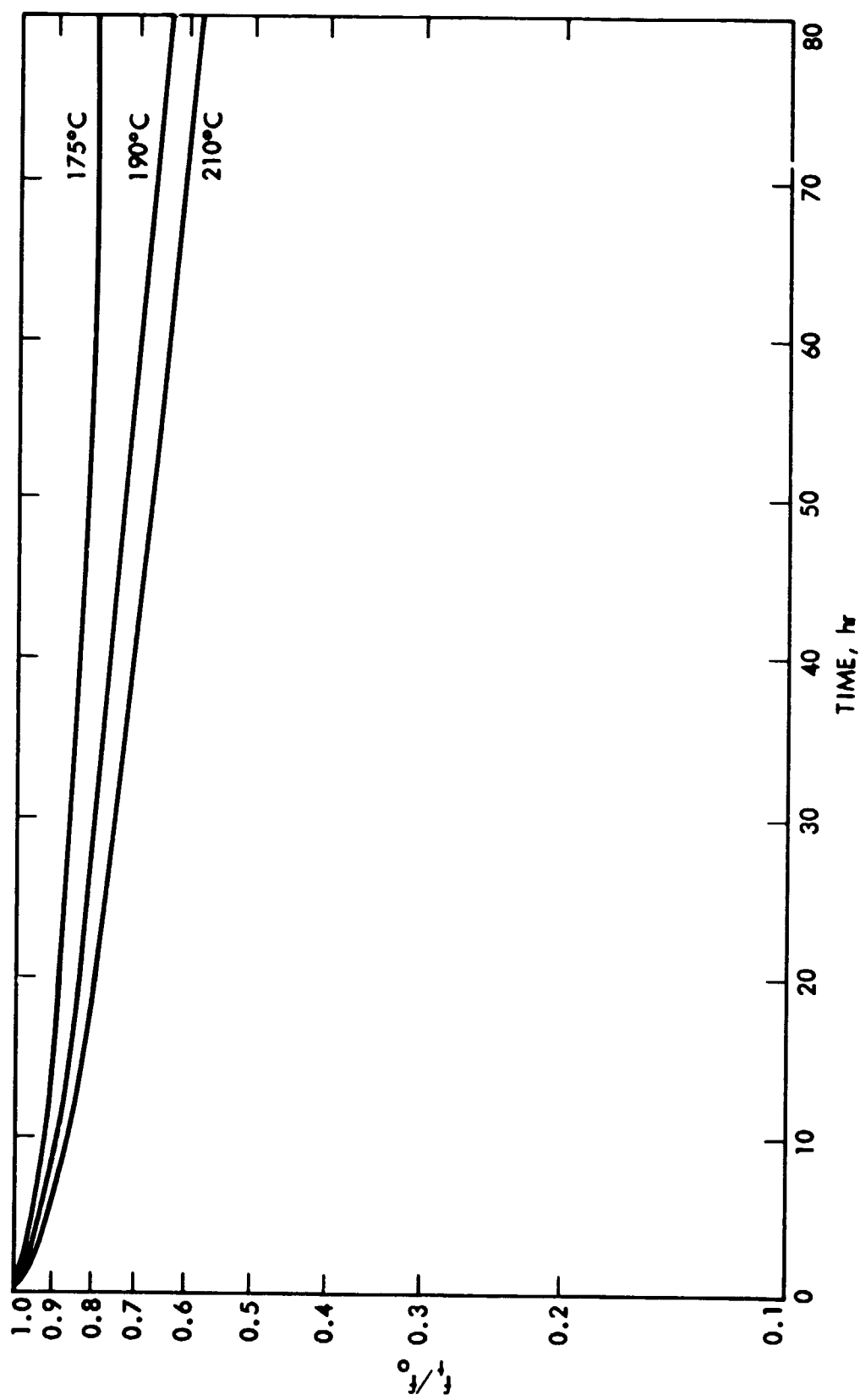Figure 13. Stress Relaxation of FVMQ 1 in Fuel I

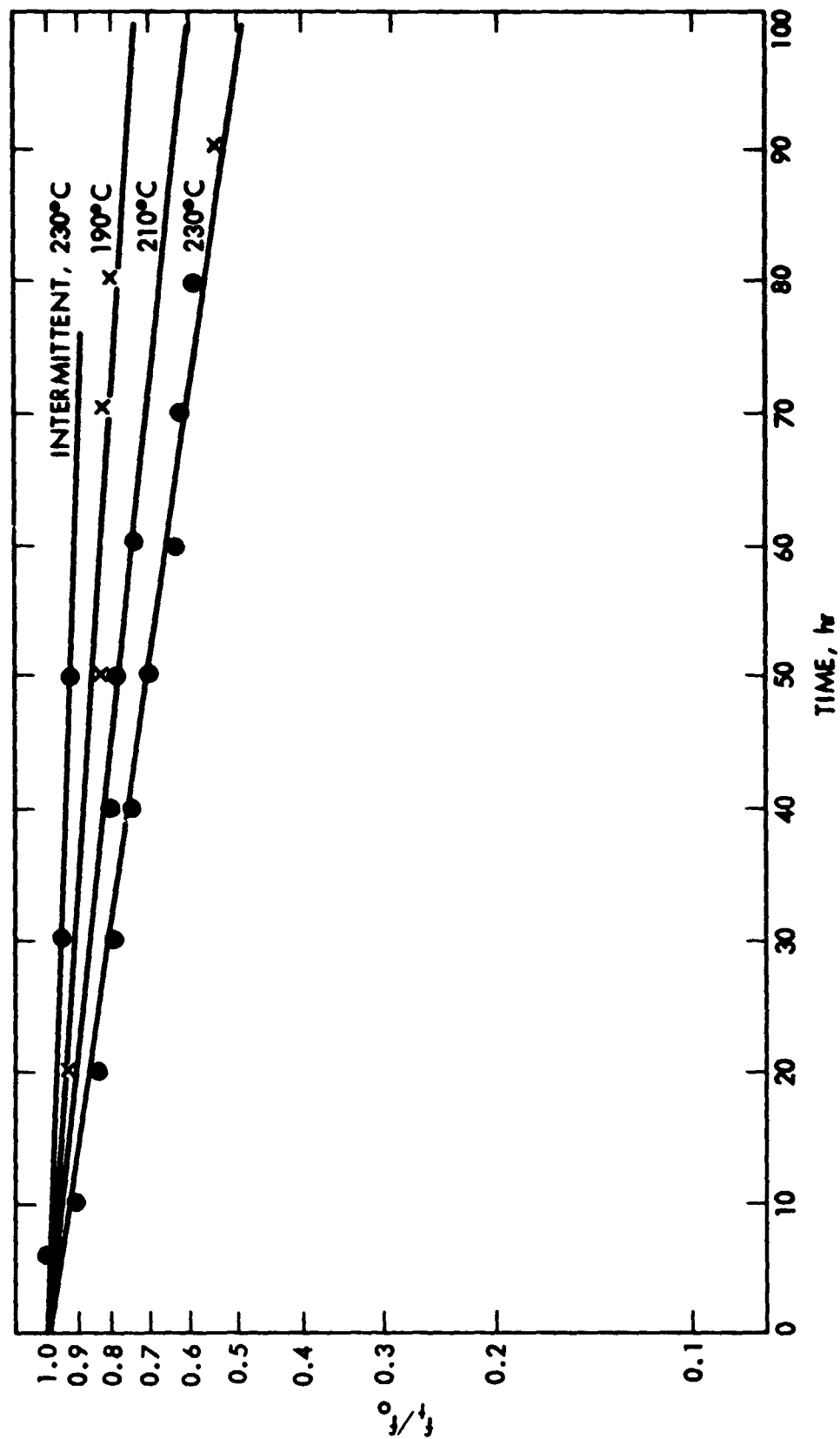Figure 14. Stress Relaxation of FVMQ 2 in Fuel I

Figure 15. Stress Relaxation of FVMQ 3 in Fuel I

The closeness of the stress relaxation curves of FVMQ with various cross-link densities shown in Figure 16 (compared, for example, with NBR data shown in Figure 4) suggests that scission at the cross-links of the network is predominant when aged in Fuel III at 150°C. This contention was confirmed by sol-gel measurements as discussed below.

Continuous and intermittent runs with FVMQ 2 in Fuels I and III at 150°C are shown in Figure 17. That of FVMQ 2 in Fuel I at 210°C is shown in Figure 18. The closeness of the intermittent and continuous curves in each case indicates that very few additional network chains, ν_e, are formed under these conditions. This is also shown in Figure 8, curves 5 and 6.

3.   Stress Relaxation of NBR and FVMQ in Air and Nitrogen

The stress relaxation of both NBR and FVMQ was also measured in air and nitrogen as "reference standards" to which runs in the fuels could be compared. The results for NBR 3 and FVMQ 2 at 150°C in air, are shown in Figures 7 and 17, respectively; those for FVMQ 3 in air and nitrogen at 250 and 275°C are shown in Figure 19. At 150°C for both NBR 3 and FVMQ 2, the reduced force of stress, f_t/f_0, increases initially and then levels off, but stays above the original stress force for the duration of the experiment. This indicates that, while the rubbers are tested at 150°C, some cross-linking of the rubber specimen occurs. At the higher temperatures, however, (Figure 19), stress relaxation curves obtained both in air and nitrogen slope downward, indicating that scission predominates cross-linking. The faster stress relaxation of FVMQ in air compared to nitrogen indicates that relaxation due to chemical changes is caused more by atmospheric oxygen than by thermal effects at the temperatures used.

4.   Activation Energies from Stress Relaxation Measurements

The temperature dependence of the SR rate constants from FVMQ 3 in Fuel III, NBR 3 in Fuels I and III, and NBR 2 in Fuel I are

26
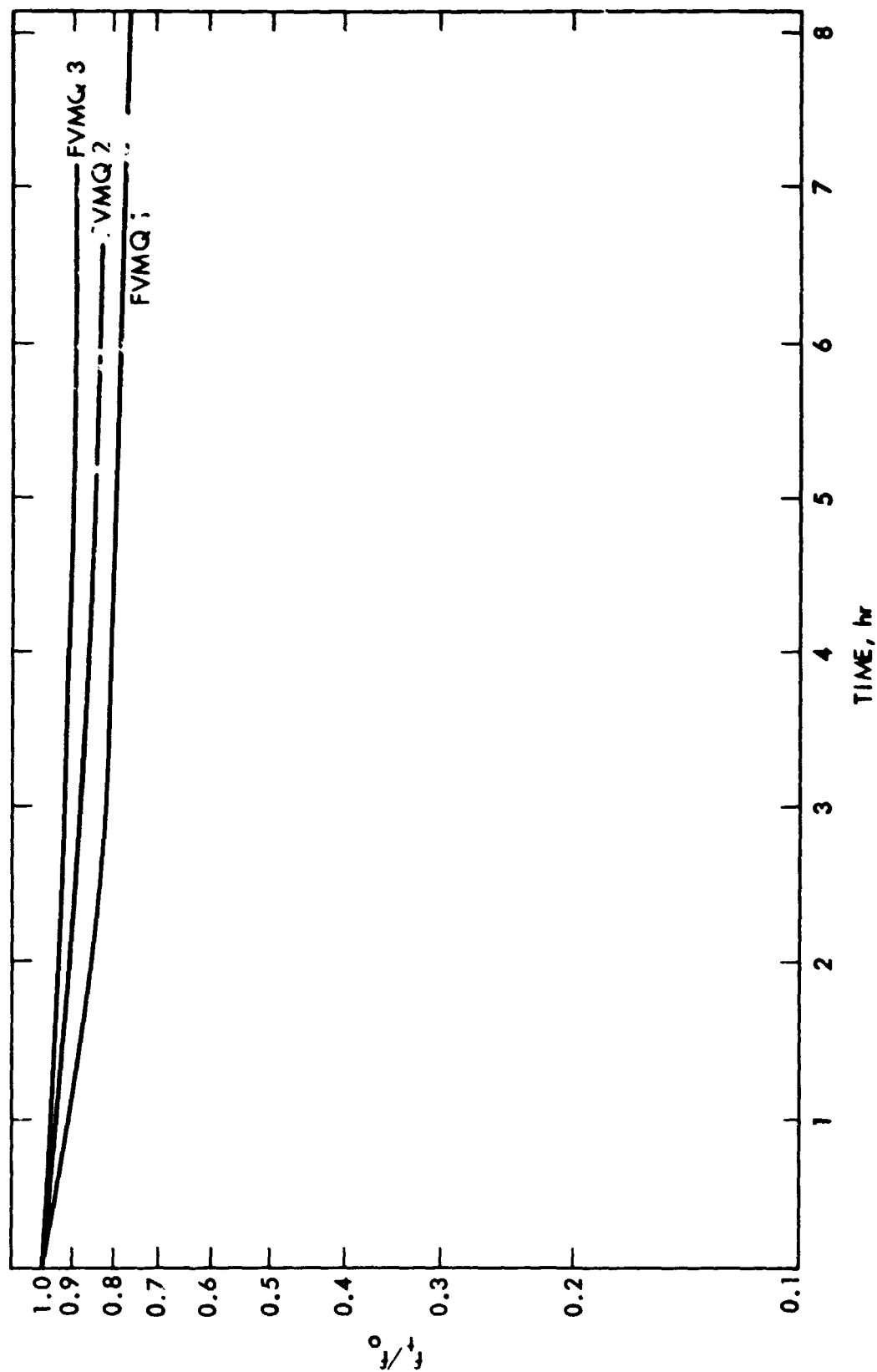
Figure 16. Stress Relaxation of FVMQ of Various Cross-link Densities at $150°C$ in *Fuel III*
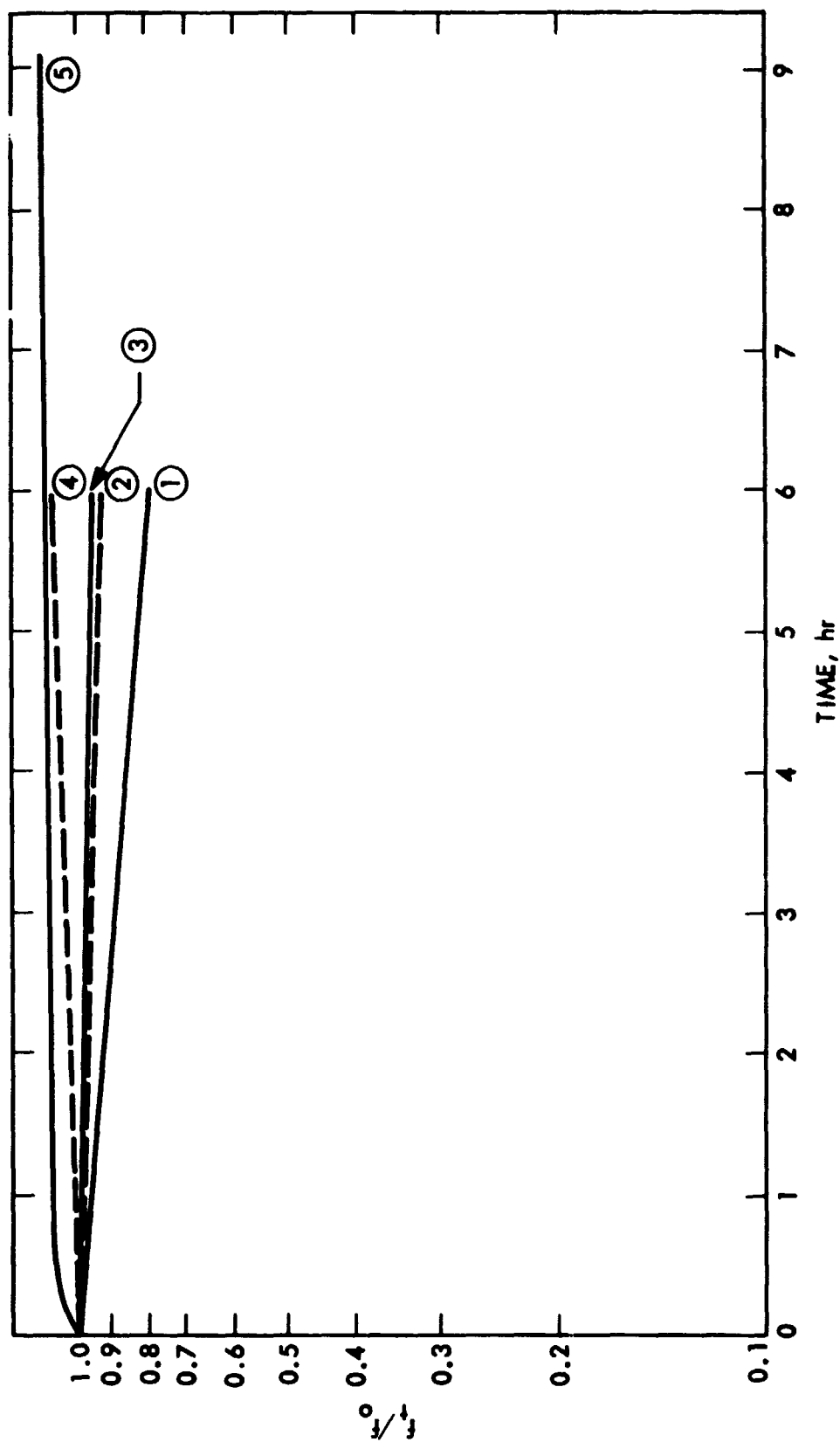
Figure 17. Stress Relaxation of FVMQ 2 at 150°C. ① In Fuel III, Continuous; ② In Fuel III Intermittent; ③ In Fuel I, Continuous; ④ In Fuel I, Intermittent; ⑤ Air, Continuous
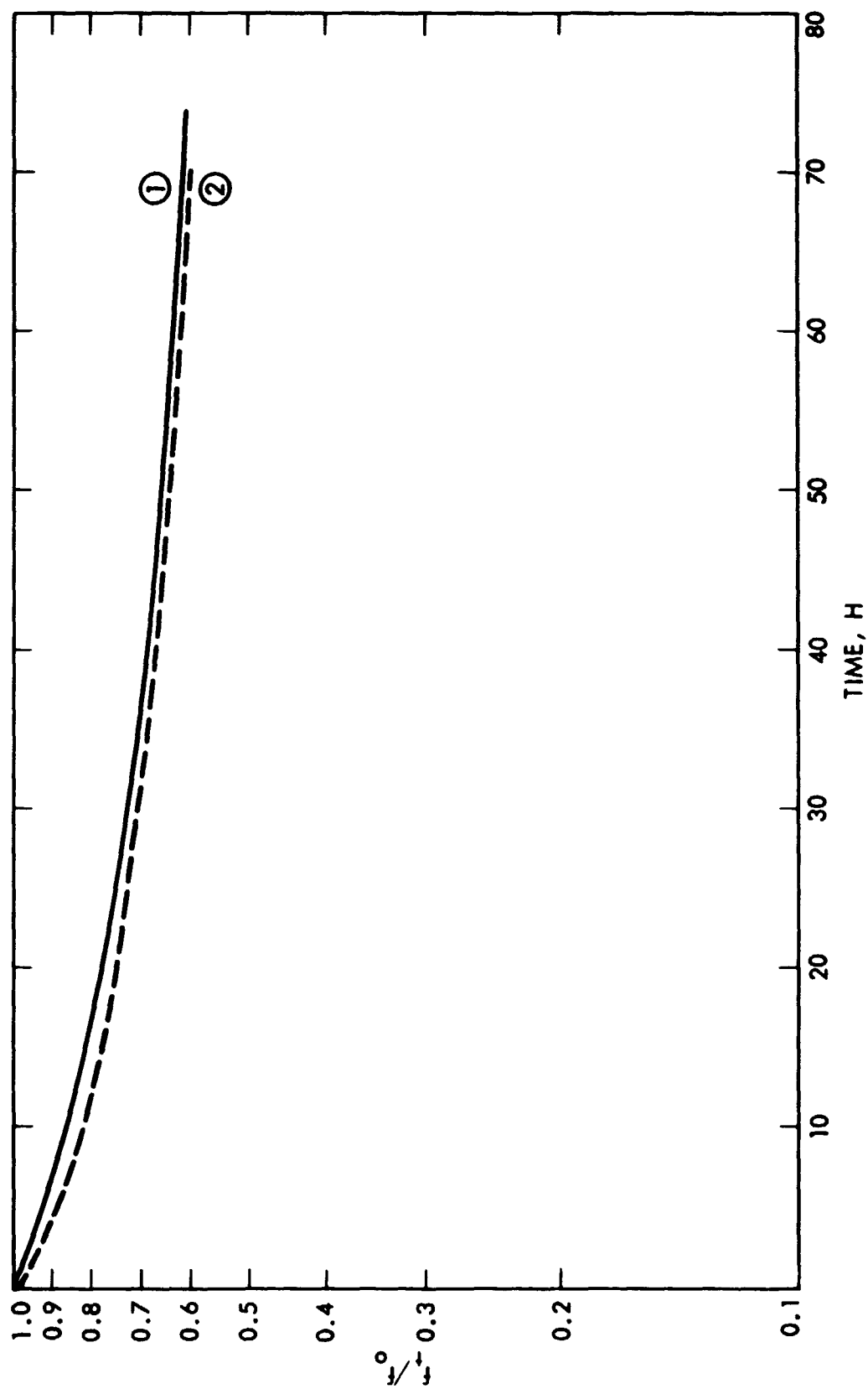
Figure 18. Continuous ① and Intermittent ② Stress Relaxation of RVMQ ② in Fuel I at 210°C
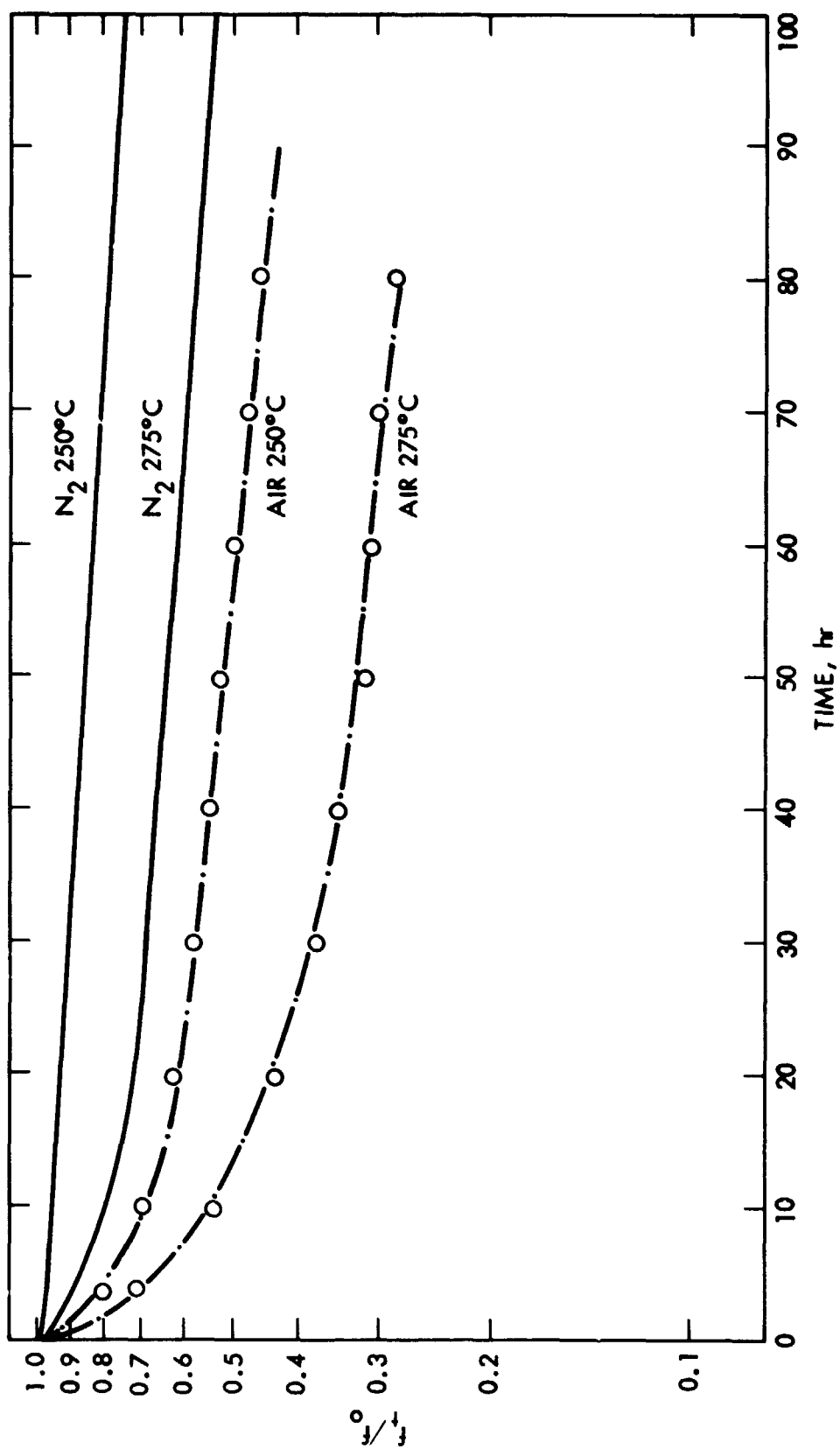
29

Figure 19. Comparison of Stress Relaxation Behavior of FVMQ 3 in Air and Nitrogen

30

shown in Figure 20. The rate constants were set to equal $1/\tau$, where τ equals time to relax a definite percentage. These values ranged from 15% for FVMQ 3 in Fuel III to 70% for NBR 3 in Fuel III. Notice the lower activation energies obtained for NBR 3 in Fuel III and NBR 2 in Fuel I. The E_a of NBR 2 in Fuel III was calculated to be a low 22.8 KJ. An Arrhenius curve for this case is not shown because data points fall outside the range of Figure 20.

5.   Extrapolation of Chemical Stress Relaxation Data for
        an Approximate Estimate of Service Life

In the temperature ranges explored, it is seen that the materials tested obey Arrhenius' law. Although it is recognized that it is hazardous to extrapolate rates to lower temperature, the results have been extrapolated as approximate estimates of service life, and as an indication of the much greater expected stability of FVMQ relative to NBR at lower use temperatures. The curves in Figure 21 were obtained by superposing the stress relaxation curves obtained at various temperatures. Thus, to plot a curve, shift factors, log K or log t^{-1}, were obtained by shifting along the logarithmic time axis the f_t/f_o vs. log t curves obtained at different temperatures, over that obtained at the reference temperature. The quantity, t, is the time it should take to obtain the same amount of stress relaxation as at the reference temperature. The extent of stress relaxation at the reference temperatures is shown in Table 2.

The times indicated on the curves in Figure 21 were obtained by drawing lines from the time axis (ordinate) to the particular curve and intercepting them with lines drawn from the desired temperatures on the temperature axis (abscissa). It should be remembered that the time axis represents reciprocal time to the percent stress relaxation values shown in Table 2. For example, the results indicate it would take 8 hours at 100°C for NBR 2 in Fuel I (curve 1, Figure 21) to relax 15%, or 26 days at 25°C to relax to the same extent. Similarly, extrapolati.1 indicates it would take more than 1000 years for FVMQ 3 in Fuel I at 100°C to relax 20% which indicates the much greater relative stability

31
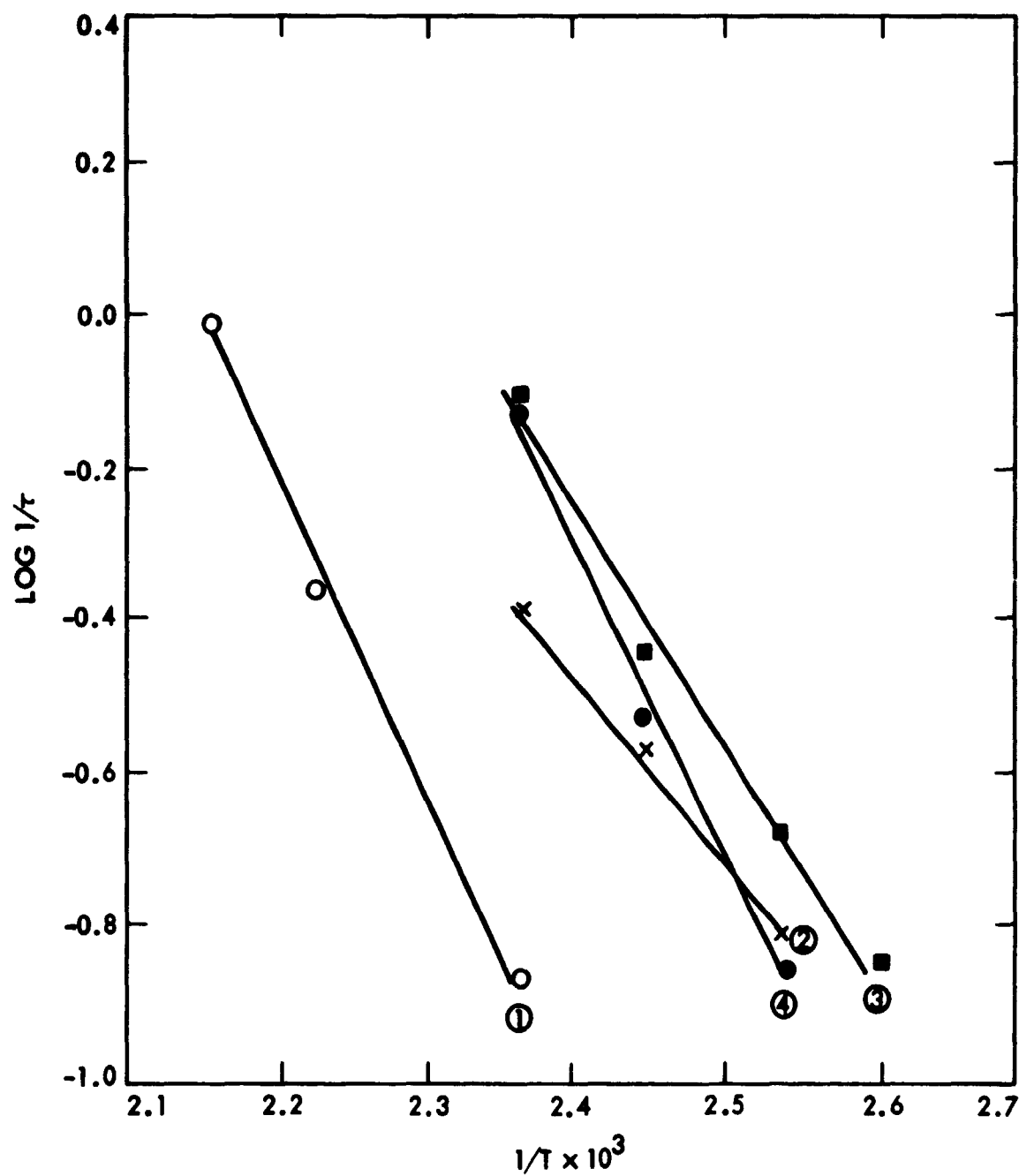
Figure 20. Temperature Dependence of Stress Realization Rates ① FVMQ 3 in Fuel III, E_a = 79.8 KJ; ② NBR 3 In Fuel III, E_a = 46.0 KJ; ③ NBR 2 in Fuel I, E_a = 57.5 KJ; ④ NBR 3 in Fuel I, E_a = 88.9 KJ
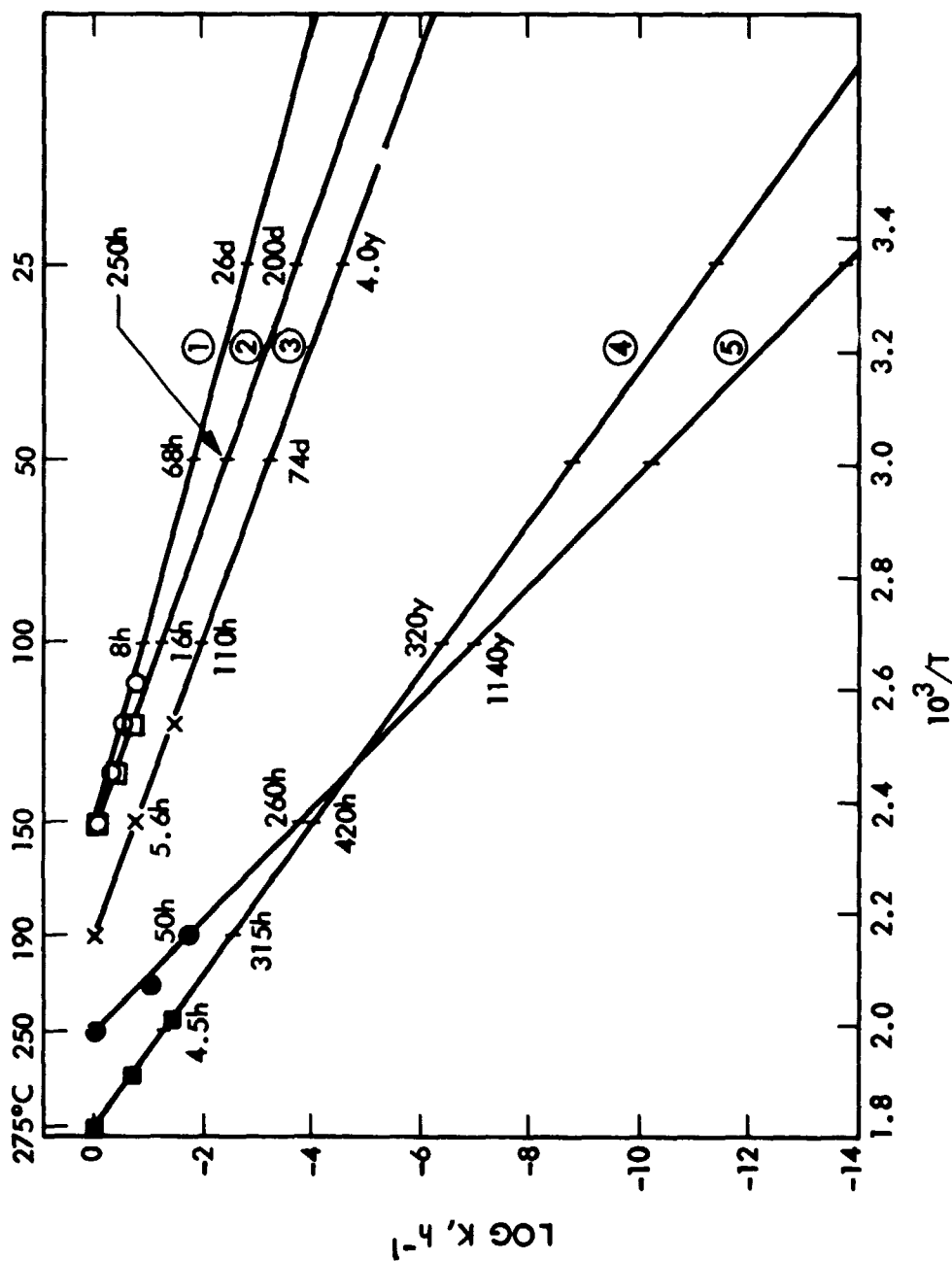
Figure 21. Temperature Dependence of Log K. Curves Obtained by Horizontal Shifting of Log K Relative to Reference Temperatures Shown. Log K = τ^{-1}; τ = Realization Time. ① NBR 1 in Fuel I; ② NBR 3 in Fuel III; ③ FVMQ 3 in Fuel III; ④ FVMQ 3 in Air; ⑤ FVMQ 3 in Fuel I

33

TABLE 2. EXTENT OF CHEMICAL STRESS RELAXATION
AT REFERENCE TEMPERATURES

Curve No. (Fig. 21)	Material	Reference Temp., °C	Extent of Stress Relaxation %
1	NBR 2 in Fuel I	150	15
2	NBR 3 in Fuel III	150	45
3	FVMQ 3 in Fuel III	190	15
4	FVMQ 3 in air	275	20
5	FVMQ 3 in Fuel I	250	20

of the fluorosilicone sealant in this fuel. The percent stress relaxations shown in Table 2 do not represent extensive chemical degradation. It would be very desirable to extend the duration of the stress relaxation experiments at lower temperatures to obtain more reliable estimates of service life.

B   SWELLING (SOL-GEL) MEASUREMENTS

Swelling measurements were made to determine the initial (unaged) cross-link densities, $\nu_{e(o)}$, the polymer-solvent interaction coefficient, χ_1, and $\nu_{e(t)}$, the cross-link density of the aged elastomers.

The $\nu_{e(o)}$ was determined using the following relationship based on the kinetic theory of elasticity:

$$\nu_{e(o)} = \frac{f(\Delta l)}{3A\ RT} \qquad (4)$$

where f = stress force, Δl = change in length of specimen, A = dry unstressed area, R is the gas constant and T is absolute temperature. The $\nu_{e(o)}$ values were used in the modified Flory-Rehner equation (Ref. 4) to evaluate χ_1, the solvent-polymer interaction coefficient,

$$\chi_1 v_2^2 = -V_s \frac{\nu_{e(o)}}{g}[v_2^{1/3} - g^{2/3}\ \frac{v_2}{2}] + \ln(1-v_2) + v_2 \qquad (5)$$

where V_s = molar volume of solvent, g = gel fraction, and v_2 = volume fraction of the rubber in the swollen gel. The v_2 was determined by the "weight method" using the following equation.

$$v_2 = \frac{1}{1 + \left(\frac{W_s}{W_f}\right)\left(\frac{\rho_r}{\rho_s}\right)} \qquad (6)$$

where W_s = weight of solvent absorbed at equilibrium, W_r = dried weight of rubber after swelling, ρ_r = density of rubber, and ρ_s = density of solvent, which, in the present cases was n-butyl acetate. The $\nu_{e(t)}$ values could be calculated from the Flory-Rehner equation, once χ_1 for

35

each rubber was known, and g and v_2 were determined experimentally. The x_1 values were as follows:

$$FVMQ: \quad x_1 = 2.44 \ V_2 + 0.915$$
$$NBR: \quad x_1 = 4.51 \ V_2 + 1.319$$
$$T: \quad x_1 = 0.5590$$

The $v_{e(o)}$ values from swollen stress measurements are shown in Table 1, together with the v_e of aged materials.

Aging was carried out in fuels I and III. NBR 2 and T-1 were aged at 140, 150 and 160°C, and FVMQ at 150, 160, 190, and only in Fuel I at 230-290°C. Ring samples were placed in sealed stainless steel tubes. Samples were withdrawn periodically and their cross-link densities were calculated from swelling and stress-strain data obtained (Table 1). It was observed that T-1 ($v_{e(o)}$ = 90.0), was degrading rapidly even in Fuel I at 140°C. After 160 hours in this environment, the gel fraction had fallen by more than 50%, indicating severe degradation. Results were worse in Fuel III. The aged samples were brittle and their tensile strength was very low or unmeasurable. The cross-link densities of the aged samples, calculated from swelling data, had fallen by as much as 82%. The temperature resistance of T in a fuel environment is evidently limited to lower temperatures.

At a later date, T-2 ($v_{e(o)}$ = 278.0), was aged at lower temperatures, namely 80, 100 and 120°C, in Fuels I and III. At these temperatures, degradation was much less severe. A slight increase in cross-link densities was observed on aging (Table 1). The gel fraction, g, decreased with time and temperature, but not as drastically as before. Plots of reduced gel fractions, g/g_0 vs. time are shown in Figure 22. The initial gel fraction, g_0, was taken as unity. The linearity of the curves indicates first-order reactions. On aging 160 h in Fuel I at 140-160°C, NBR 2 showed extensive additional cross-linking, as shown in Table 1, but substantial decrease in the cross-link density occurred after aging in Fuel III, at the same temperatures and aging period.
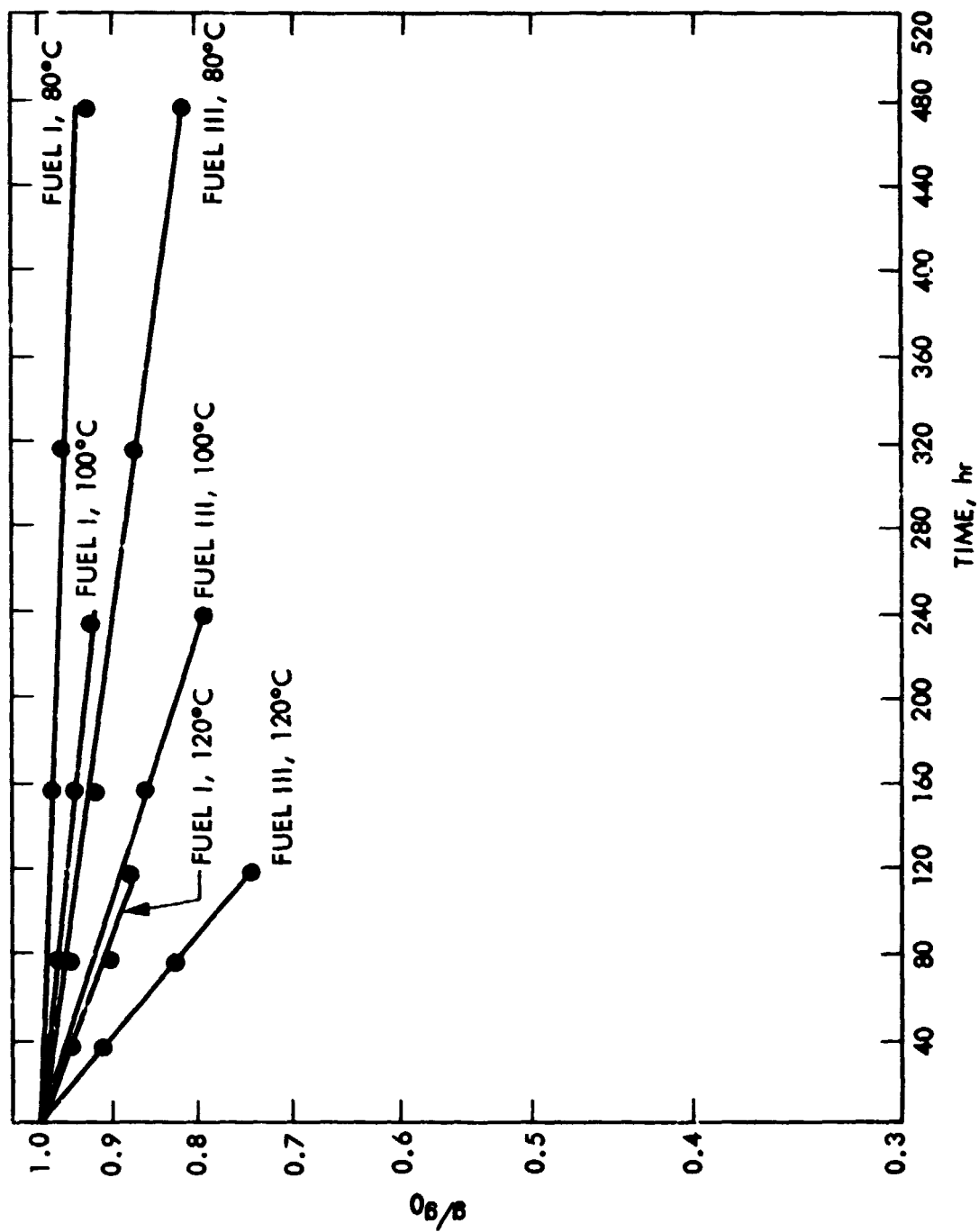
Figure 22. Dependence of Reduced Gel Fraction of Polysulfide Sealant on Time at Various Temperatures in Fuels I and III

The accelerated aging of FVMQ 3 was carried out in Fuels I and III at 150, 160 and 190°C, and only in Fuel I at 230-290°C. An experiment in Fuel I vapor is also reported. Results are shown in Table 1. Aging in Fuel III was faster than in Fuel I. For example, after 240 h exposure to Fuel III at 150°C, v_e decreased from 240 to 137 moles/m^3, whereas it had decreased to 161 moles/m^3 in Fuel I. The same pattern was observed at 160 and 190°C. Degradation, as manifested by the decrease in v_e, increased with temperature as expected. For example, after 200 h in Fuel I at 230°C, the v_e decreased from 200 to 100 moles/m^3, but to 43 moles/m^3 at 250°C. Compared with the action of Fuel I vapor on FVMQ 3, the effect of liquid Fuel I in the sealed container was much more severe. After 300 h in liquid Fuel I at 60°C and 2500 h in Fuel I vapor at 227°C, the decrease in v_e was less than 6% (from 21.1 to 19.9 moles/m^3), whereas in liquid Fuel I at 230°C after only 200 h, the decrease was 50%, and after 1000 h, 96%.

The extensive degradation in the confined liquid Fuel I could be explained thusly: both the fluorosilicone backbone chain and the cross-links contain siloxane bonds, Si-O, with reported bond energy ranging from 369 KJ/mol (ref. 5) to 489 KJ/mol (ref. 6). Although these values represent strong bonds, the nearly 40% ionic character (refs. 7, 8) of the siloxane bond makes it susceptible to nucleophilic and electrophilic attack by basic and acidic degradation products that may have formed during the thermal breakdown of either fuel and fluorosilicone polymer, or by impurities, such as polymerization catalysts present initially. Any such substance formed in the FVMQ or present to start with, may have been washed away by the fuel vapor from the reaction zone. If damaging tar containing acidic and basic components was formed by the thermolysis of Fuel I, they would probably not be volatile enough at the test temperature to reach the FVMQ while exposed to fuel vapor, but would be in intimate contact with it during the liquid fuel exposure.

Swelling or sol-gel determinations can also yield information about the site of cleavage in the polymer. Horikx (Ref. 9) showed that the following relationships hold for random scission, equation (7), and cross-link scission, equation (8):

$$\frac{\nu_{e(t)}}{\nu_{e(o)}} = \frac{(1-S^{1/2})\ (1-S)}{(1-S_o^{1/2})^2\ (1-S_o)} \tag{7}$$

$$\frac{\nu_{e(t)}}{\nu_{e(o)}} = \frac{S_o^{1/2}(1+S_o^{1/2})\ (1-S^{1/2})^2}{S^{1/2}(1+S^{1/2})\ (1-S_o^{1/2})^2} \tag{8}$$

where S_o and S are sol fractions of unaged and aged materials, respectively. The curves for these equations are shown in Figure 23, together with the plots for the data obtained from T-1 aged in Fuel III (curve 3), and FVMQ 3 aged in Fuel I (curve 4). Curve 1 represents the response predicted for random chain scission, equation (7), while curve 2 represents the response predicted for cross-link scission, equation (8). The shape of curve 3 is similar to that of curve 1, suggesting that scission takes place randomly in the backbone chain of T. The plot for FVMQ 3 (curve 4), is unmistakably similar to curve 2 and confirms the results suggested from stress relaxation measurements that scission in FVMQ is predominant at the cross-links. The gel fractions of NBR changed so slightly on aging that Horikx curves could not be plotted.

C.   MEASUREMENT OF MECHANICAL PROPERTIES

Extensive stress-strain measurements were made on unaged NBR and FVMQ compositions. Mechanical testing of T was limited to one cross-link density material aged in Fuels I and III at 80, 100 and 120°C The relative stress at break of these samples vs. aging time are plotted in Figure 24. The temperature dependence of the aging rate is shown in Figure 25. Here, t for cases 1 and 2 is the time it takes for g/g_0, the relative gel fraction, to decrease 5%; for cases 3 and 4, it is the time necessary for the stress to decay 40 and 70%, respectively. Activation energies obtained from temperature dependence of aging rate measured from the change in gel fractions, g, were higher than those obtained from the temperature of the aging rate as measured from the change in σ_b.
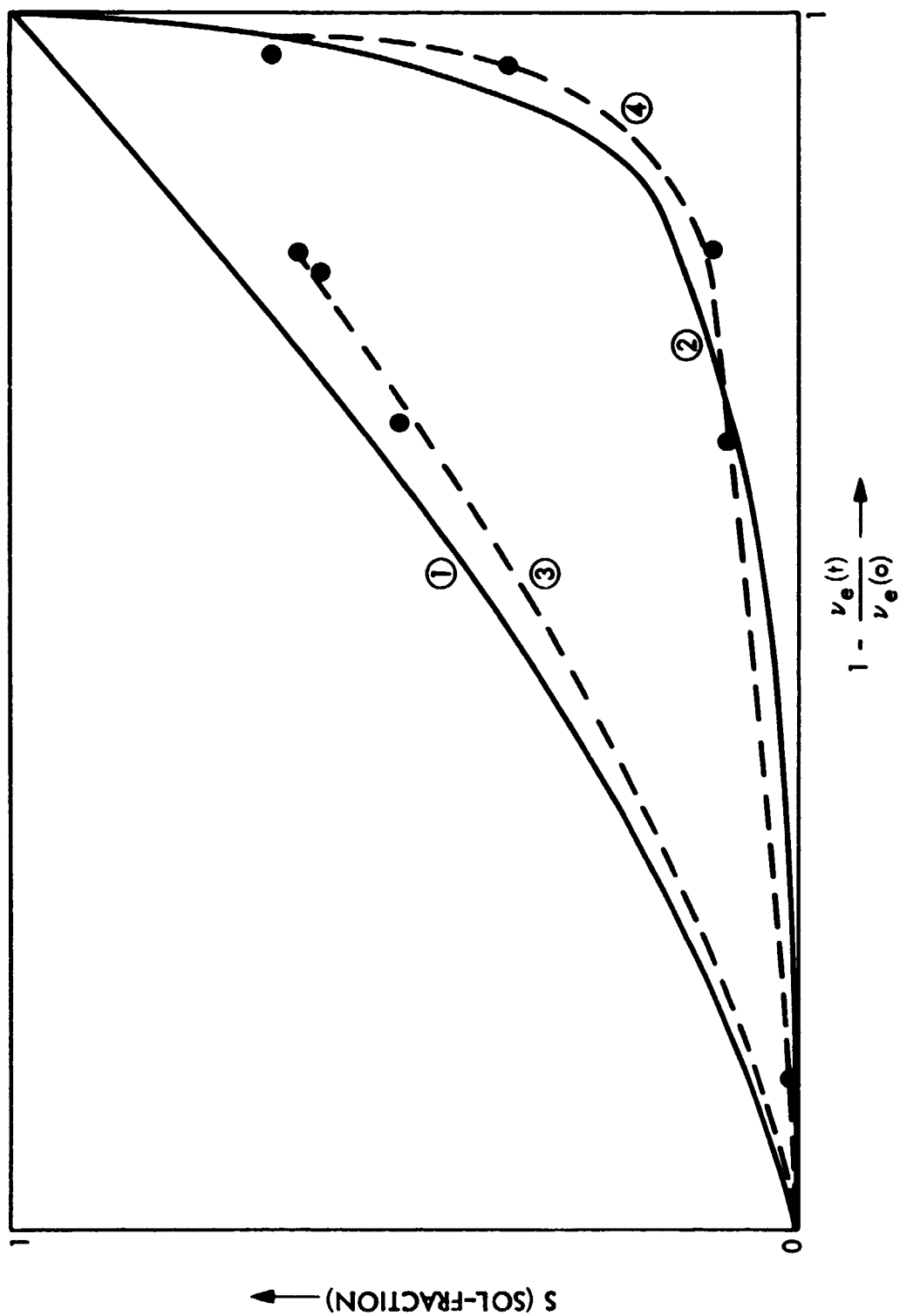
39

Figure 23. Sol-Gel Relationship. ① Theoretical Curve for Random Chain Scission; ② Theoretical Curve for Cross-link Scission; ③ Experimental Curve for T-1 in Fuel III; ④ Experimental Curve for FVMQ 3 in Fuel I

40
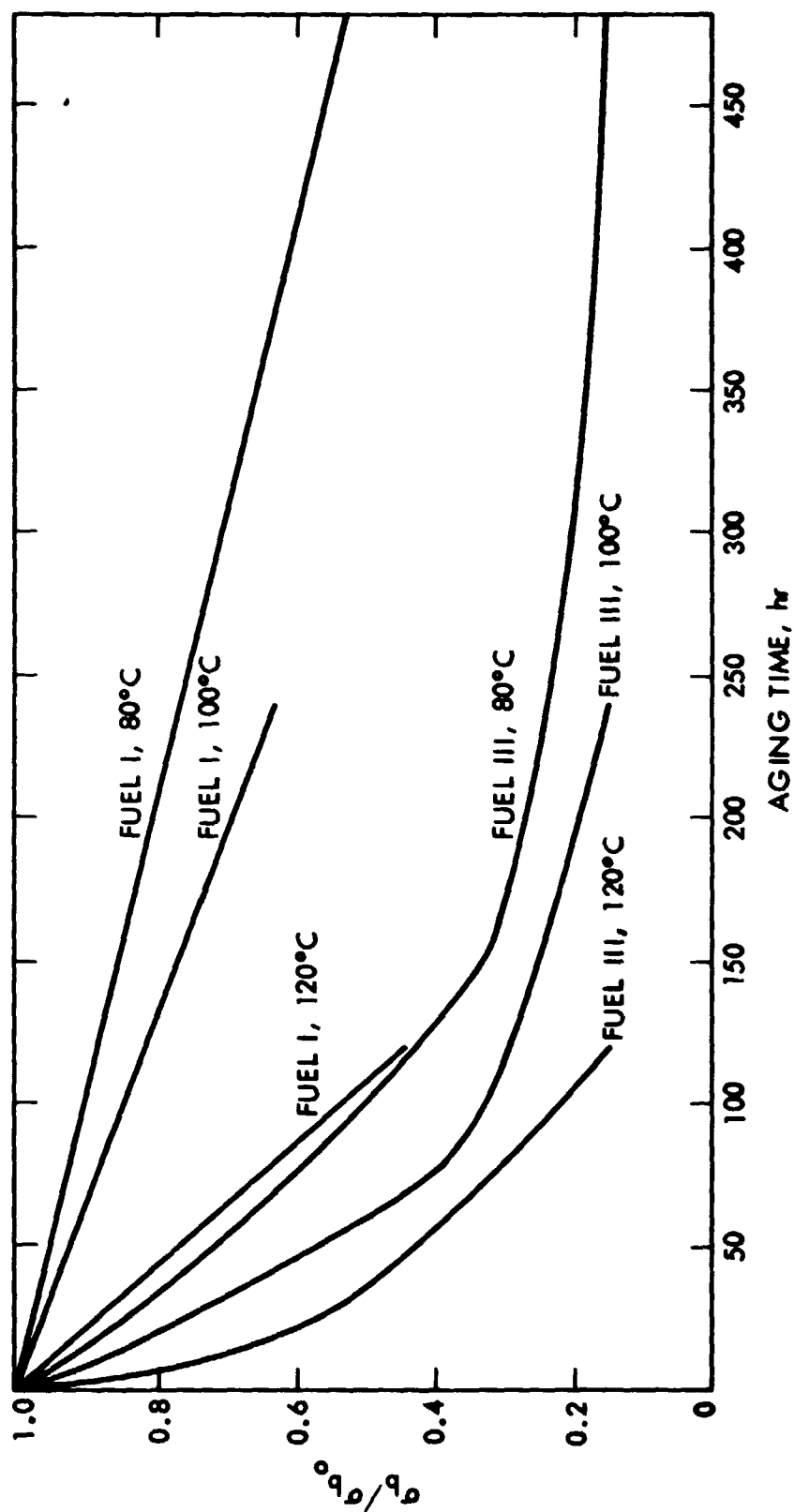
Figure 24. Dependence of Reduced Stress at Break, σ_b/σ_{b_o}, on Aging Time for Poly-sulfide Sealant T-1 at Various Temperatures, in Fuels I and III

41

Figure 25. Temperature Dependence of Tensile Stress Decay Rate and Change in Gel Fraction of Polysulfide T-1 in Fuels I and III. (1) In Fuel I, E_a, 56.7 KJ (From Change in Gel Fraction) (2) In Fuel III, E_a, 49.2 KJ (From Change in Gel Fraction); (3) In Fuel I, E_a, 47.9 KJ (From Stress Decay); (4) In Fuel III, E_a, 37.9 KJ (From Stress Decay)

42

The purpose of the dynamic mechanical testing of the unaged rubbers was to establish a basis for the prediction of the long-time behavior of these elastomers. This approach is based on the existence and ap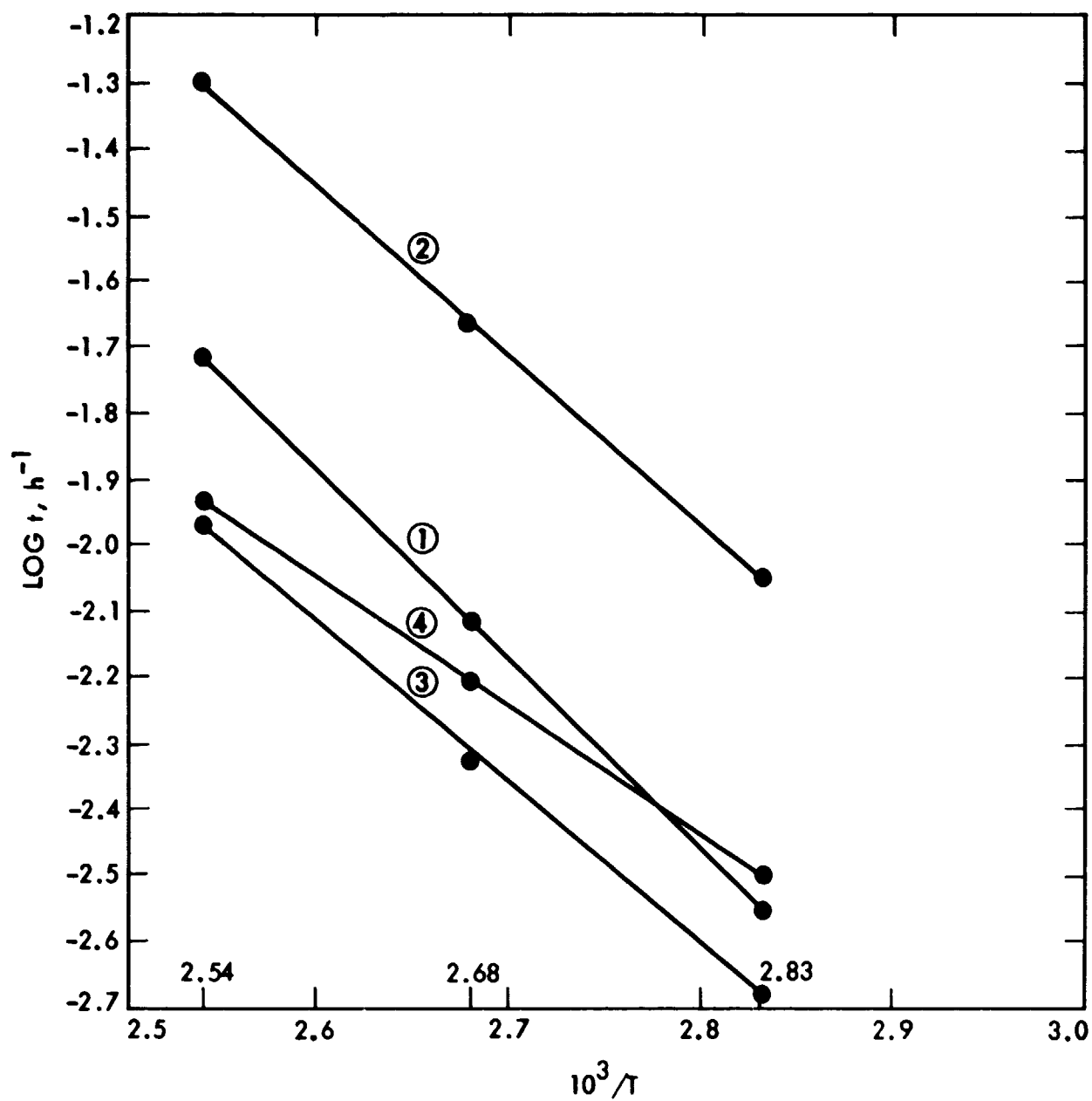proximate invariance of the tensile property surface. A typical tensile property surface for a Viton B[1] elastomer is shown in Figure 26. The concept of the property surface is based on the fact that the mechanical response of an elastomer can be considered in terms of these variables: stress, σ; strain, ε; and time, t. The effect of temperature is incorporated into the time scale by the relationship $\log t/a_T$, where the value of $\log a_T$ is the experimentally-determined, time-temperature shift factor. The development of the tensile property surface which relates these parameters by a single analytic surface with a single rupture failure boundary is described in Ref. 10.

The surface is conveniently generated by measuring the uniaxial stress-strain response of the given elastomer as a function of strain rate and temperature. Typically, it is necessary to test the elastomer at about 10 different strain rates at each of 10 to 15 test temperatures. Although this represents a considerable expenditure of time and effort, knowledge of the surface is of fundamental importance in understanding and predicting the mechanical response of an elastomer.

The response of an elastomer to any uniaxial input will simply be a path traced out on the surface. For example, the path traced out during a creep experiment (i.e., constant load) starting at point A in Figure 26 and terminating at the point B, will be the curve AB, which is generated by the intersection of this surface with a plane parallel to the strain-time plane and which passes through both A and B. The projection of this path to the strain-time plane is depicted by the lower curve AB: this latter curve corresponds to creep data as normally plotted. Similar consideration can be used for experiments carried out under other test modes. Thus, the path traced out on the surface by a stress relaxation (i.e., fixed strain) experiment carried out by starting from the same point A used for the creep experiment is shown in Figure 26 as the curve AC.

---

[1] Registered trademark of E.I. duPont deNemours & Co., Inc.

Figure 26. Tensile Property Surface for Viton B® Elastomer
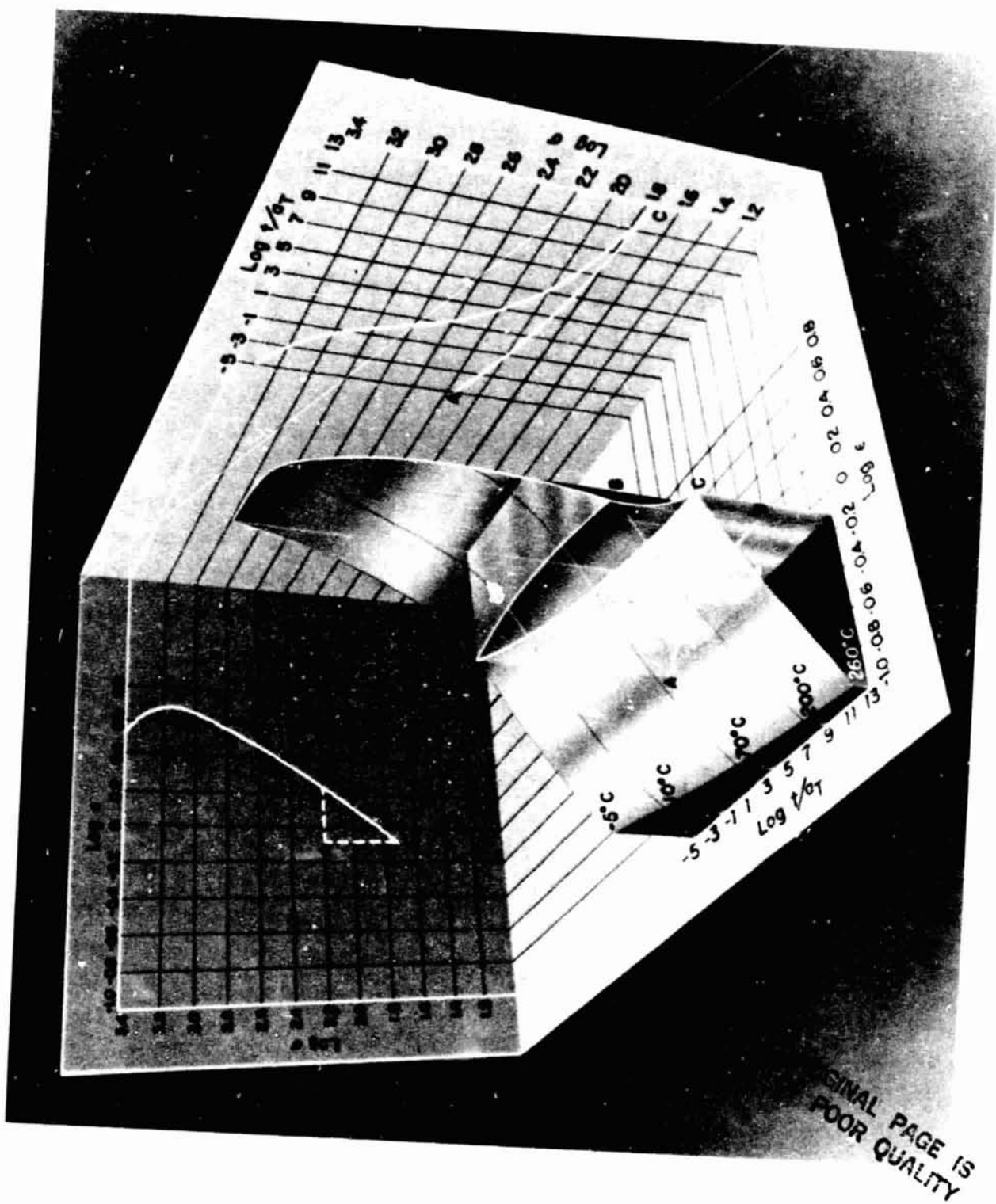
Rupture on this surface is represented graphically as discontinuity or boundary which can be considered to result from the intersection of the physical property surface with another surface representing failure. In Figure 26, this rupture condition is represented by the terminating line on the right. Hence, the specimen undergoing creep and following the surface along path AB will break when this path intersects the boundary (at point C).

The effect of changes in the cross-link density of the elastomer on the location of the property surface has also been studied for three chemically different types of rubber, viz: a hydrocarbon, a fluorocarbon, and a fluorosilicone rubber. For all three types, the effect of a change in cross-link density is simply to change the time scale of the experiment analogously to the change in time scale observed when the temperature is changed.

The effect of the changes in the cross-link density on the time scale is given by the cross-link density-time shift factor, a_x, which is expressed by

$$\log a_x = -7.7 \log v_e + C \qquad (9)$$

where C is a constant dependent on the chemical nature of the elastomer. Thus, when temperature and cross-link density are both changed, the reduced time is $t/a_T a_x$.

1.   Biaxial Deformations

In many applications, the elastomer is subjected to biaxial deformations (e.g., flexing and folding), while the experience presented above was limited to tests carried out in uniaxial deformation. However, it can be said that the failure time in biaxial deformation can never exceed that under conditions of uniaxial deformation. Hence, the results obtained with the uniaxial test can be used to assess the promise of a candidate material. For example, if the candidate material does not have sufficient lifetime in a uniaxial test, it should not be a candidate for an application involving biaxial deformation. In this discussion, it is assumed that no chemical degradation of the elastomer has occurred.

45

2.   Analysis of the Data

The following parameters were calculated from the load-time data obtained from the Instron strip charts:

$$\frac{\sigma_b T_o}{T} = \text{tensile stress at failure (break), psi}$$

$$\varepsilon_b = \text{strain at failure}$$

$$t_b = \text{time at failure}$$

T_o and T are an arbitrary reference temperature, 298 K and T are the test temperatures, respectively.

The three NBR formulations were tested at 298, 323 and 353 K, and the three FVMQ compounds were tested at 298, 323 and 363 K. Plots of log σ_b 298/T vs. log t_b were prepared. The process is illustrated in Figure 27 where the data obtained for NBR 2 at 298, 323 and 353 K are plotted. The definitions of the plotting symbols are given in Table 3. The curve shown in Figure 28 was obtained by shifting the plots in Figure 27 horizontally, relative to the reference curve at 298 K to obtain the single response shown in Figure 28. A light table and translucent graph paper were used to carry out the shifting process. Log σ_b 298/T versus log t responses for NBR 1 and 3, and FVMQ 1, 2 and 3 were similarly obtained and are shown in Figures 29-33. In all cases, the reference temperature was 298 K.

The amount of horizontal shift is log a_T and is temperature dependent. This dependence is shown for NBR and FVMQ in Figure 34. Although there is little or no overlap of the data, the shifted curves, Figures 29-33 are believed to be valid because they agree with known data on other rubber systems.

Superposition of the failure response of NBR with different cross-link densities, ν_e (Figures 28-30), by horizontal shifting with respect to NBR 3 as reference gave the master plot shown in Figure 35. Similar treatment of the three failure data for FVMQ 1, 2, and 3 (Figures 31-33) with respect to FVMQ 3 as reference gave the master plot shown in Figure 36. The amount of the cross-link density-time shift

TABLE 3. DEFINITION OF PLOTTING SYMBOLS

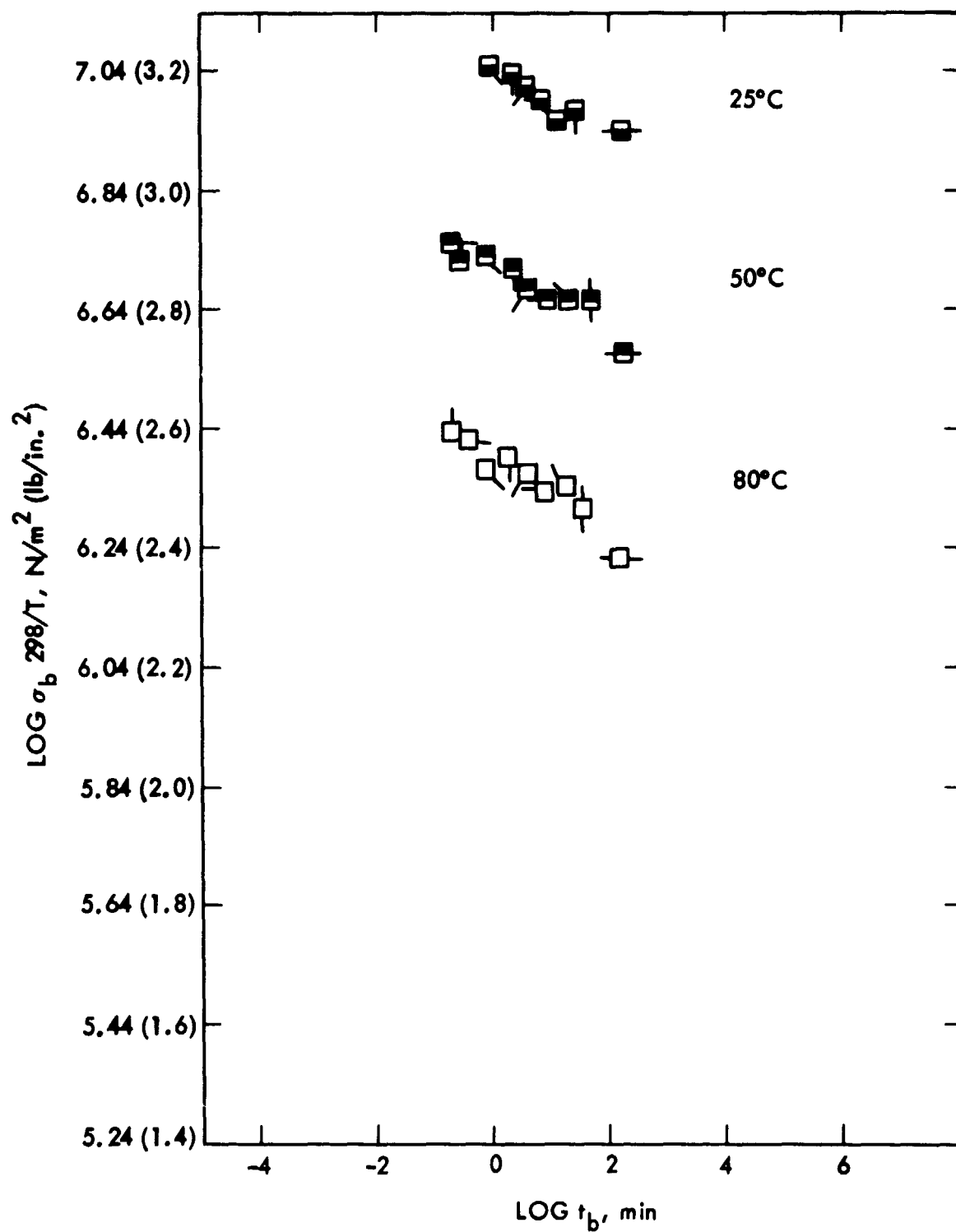| Symbol	Cross-link Density	Temperature °C	Flag	Rate in/min
△	Low (1)		♂	20
			♂	12
☐	Medium (2)		○—	10
			⚲	5
○	High (3)		♀	2
			♀	1
▲, ▬, ⬤		25	—○	0.5
			—○—	0.2
▲ ▬ ⬤		50	♀	0.1
△ ☐ ○		80 (90)		

Figure 27. Stress Rupture Data for NBR 2 at Various Temperatures
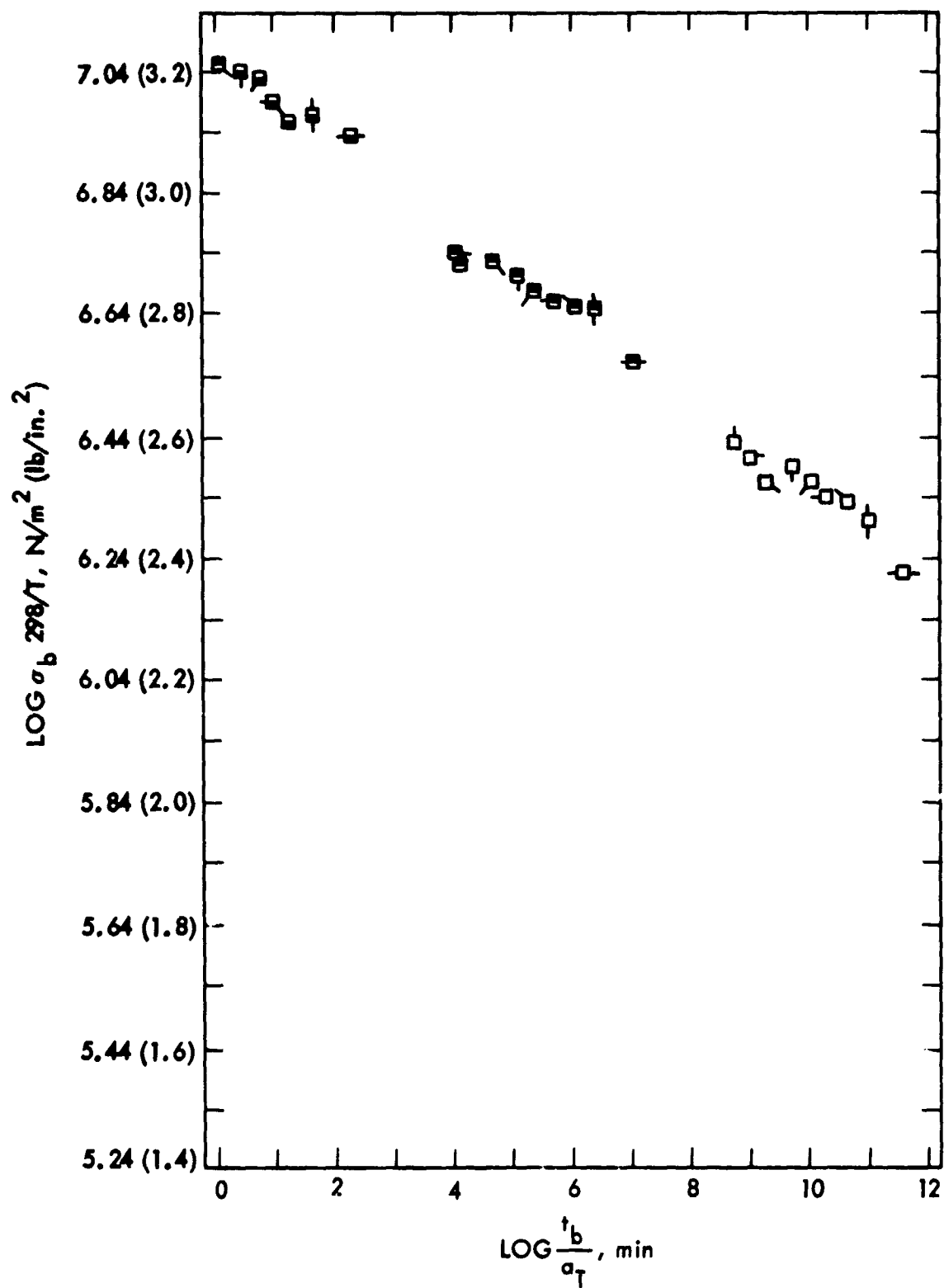
48

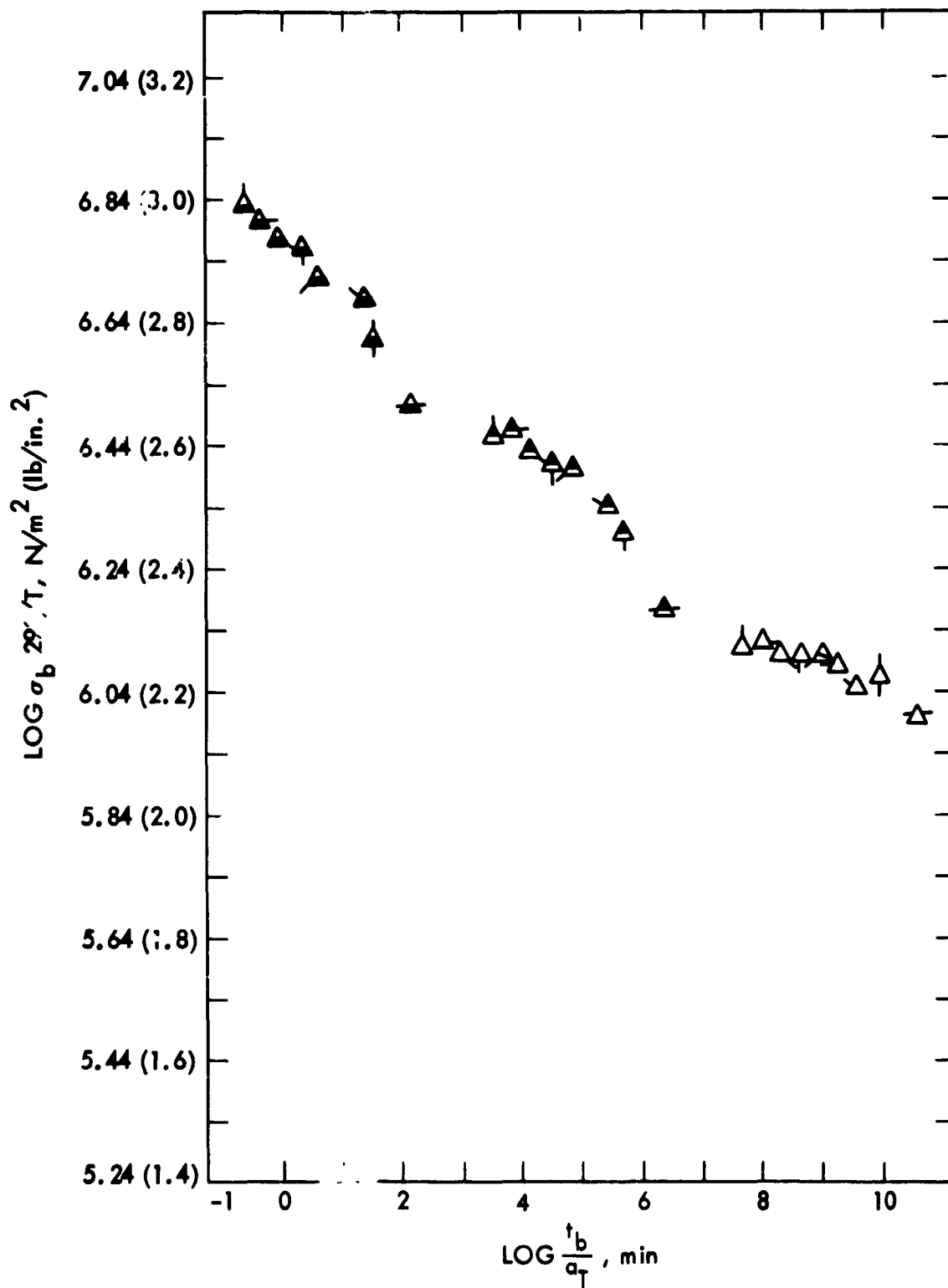Figure 28. Dependence of σ_b on t_b for NBR 2

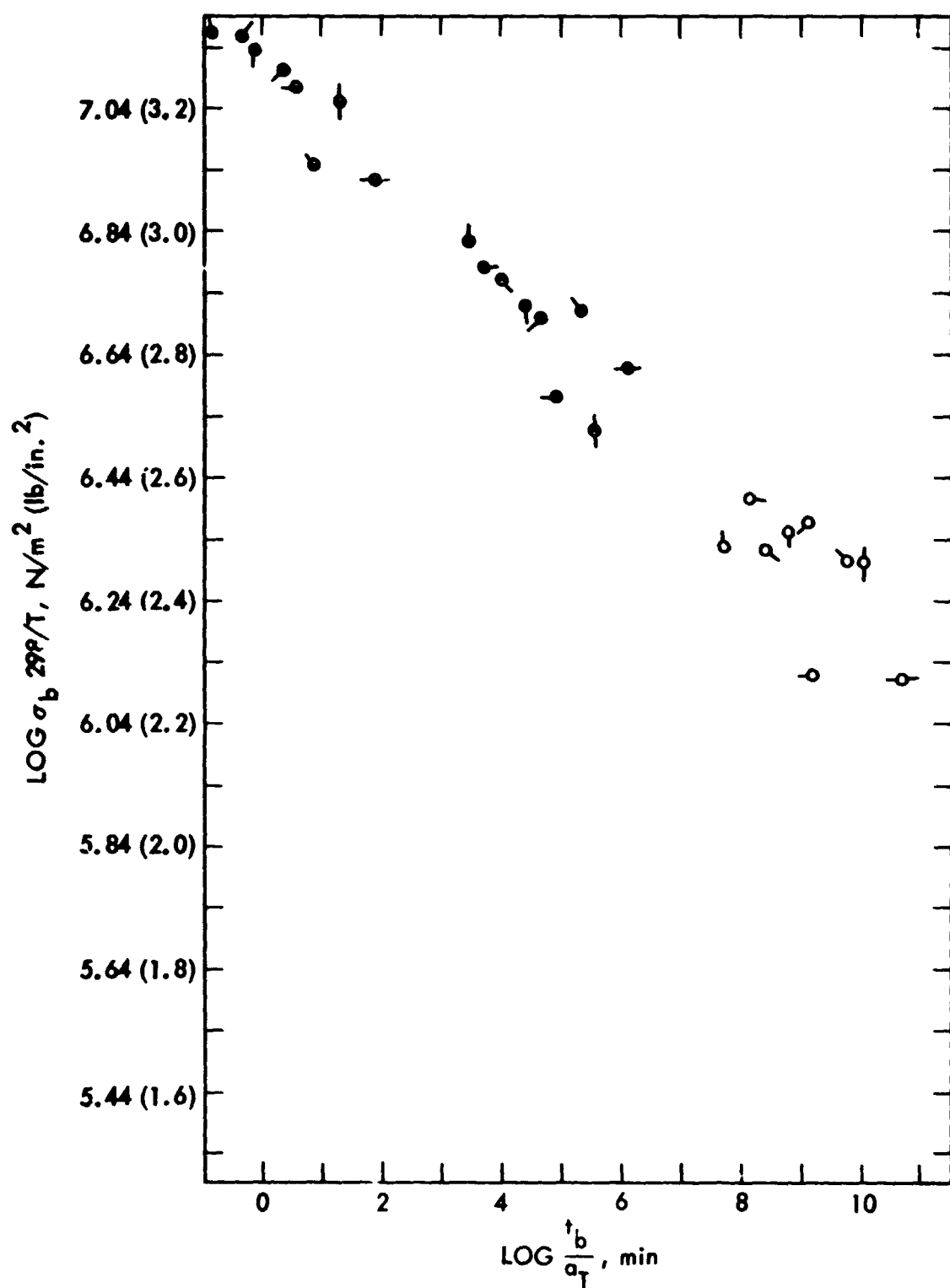Figure 29. Dependence of σ_b on t_b for NBR 1

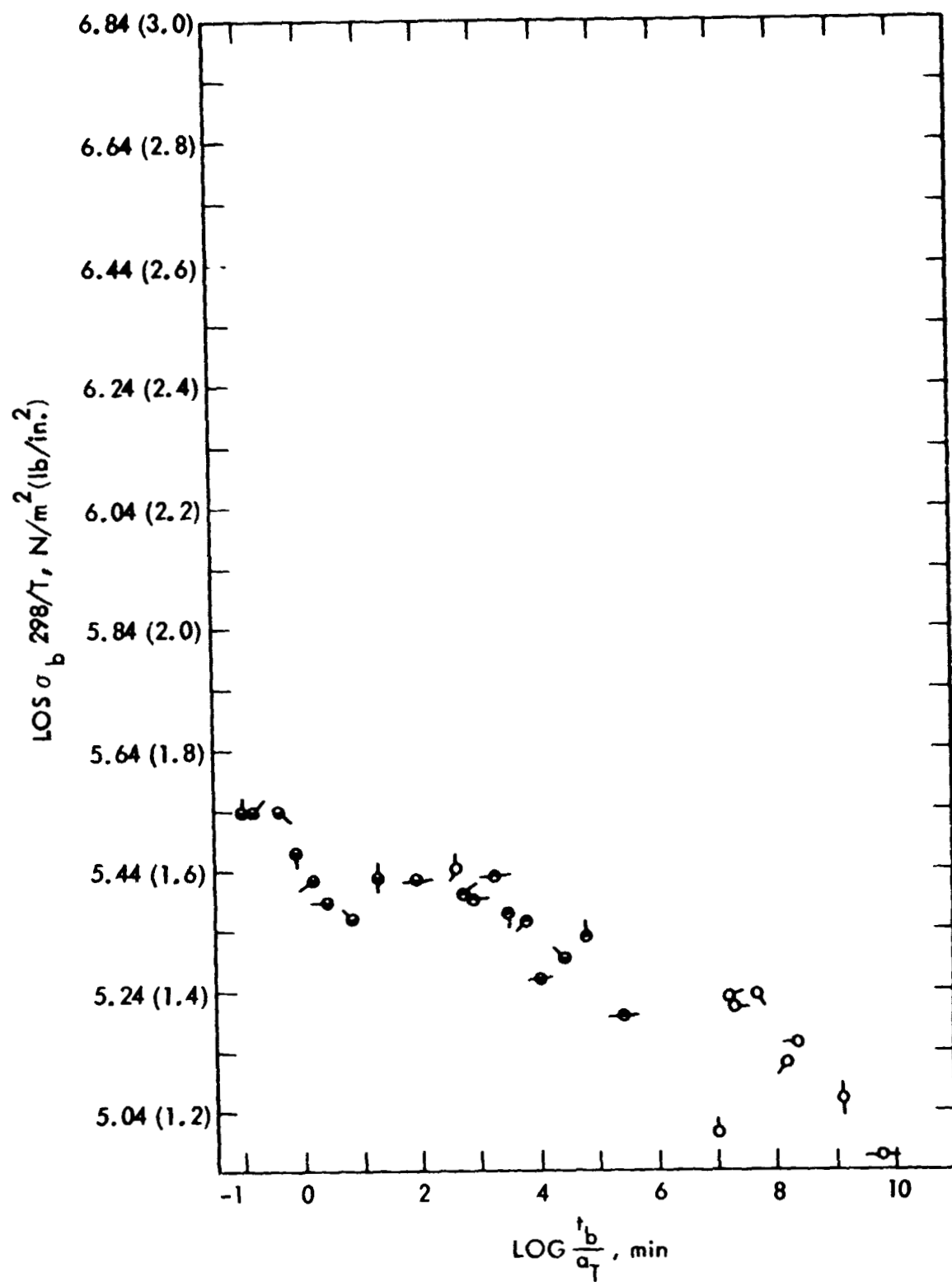Figure 30. Dependence of σ_b on t_b for NBR 3

51

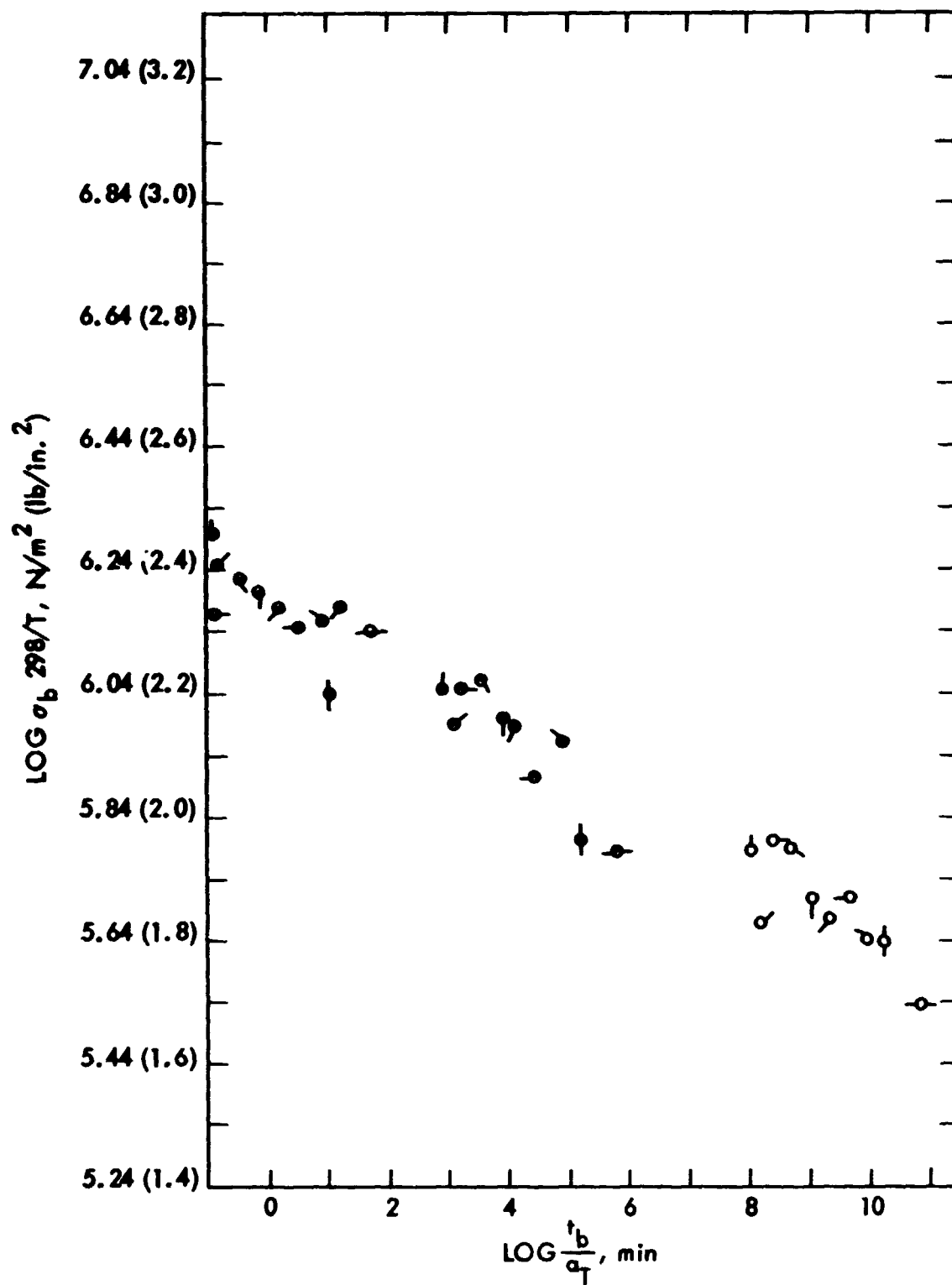Figure 31. Dependence of σ_b on t_b for FVMQ 1

Figure 32. Dependence of σ_b on t_b for FVMQ 2
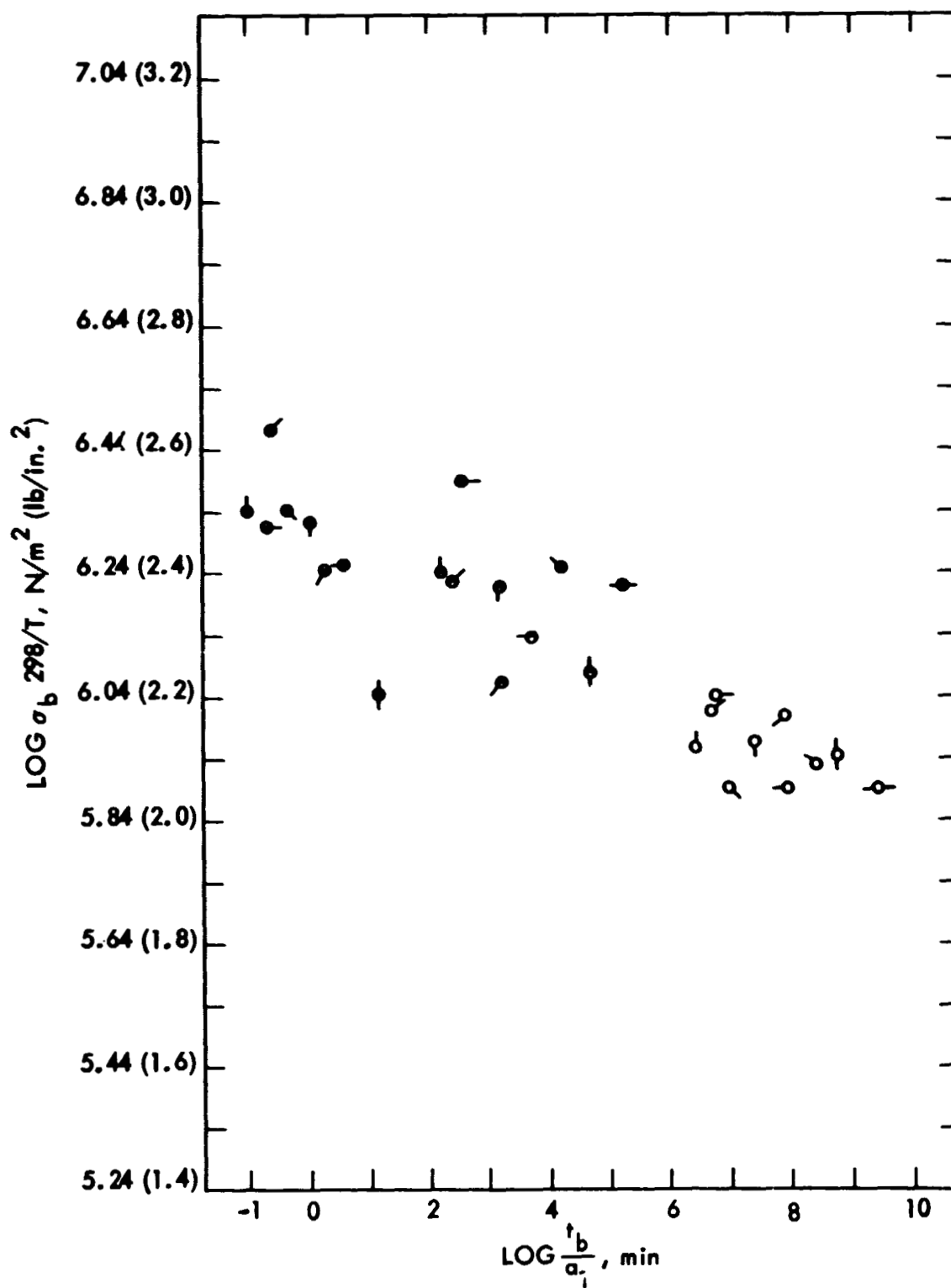
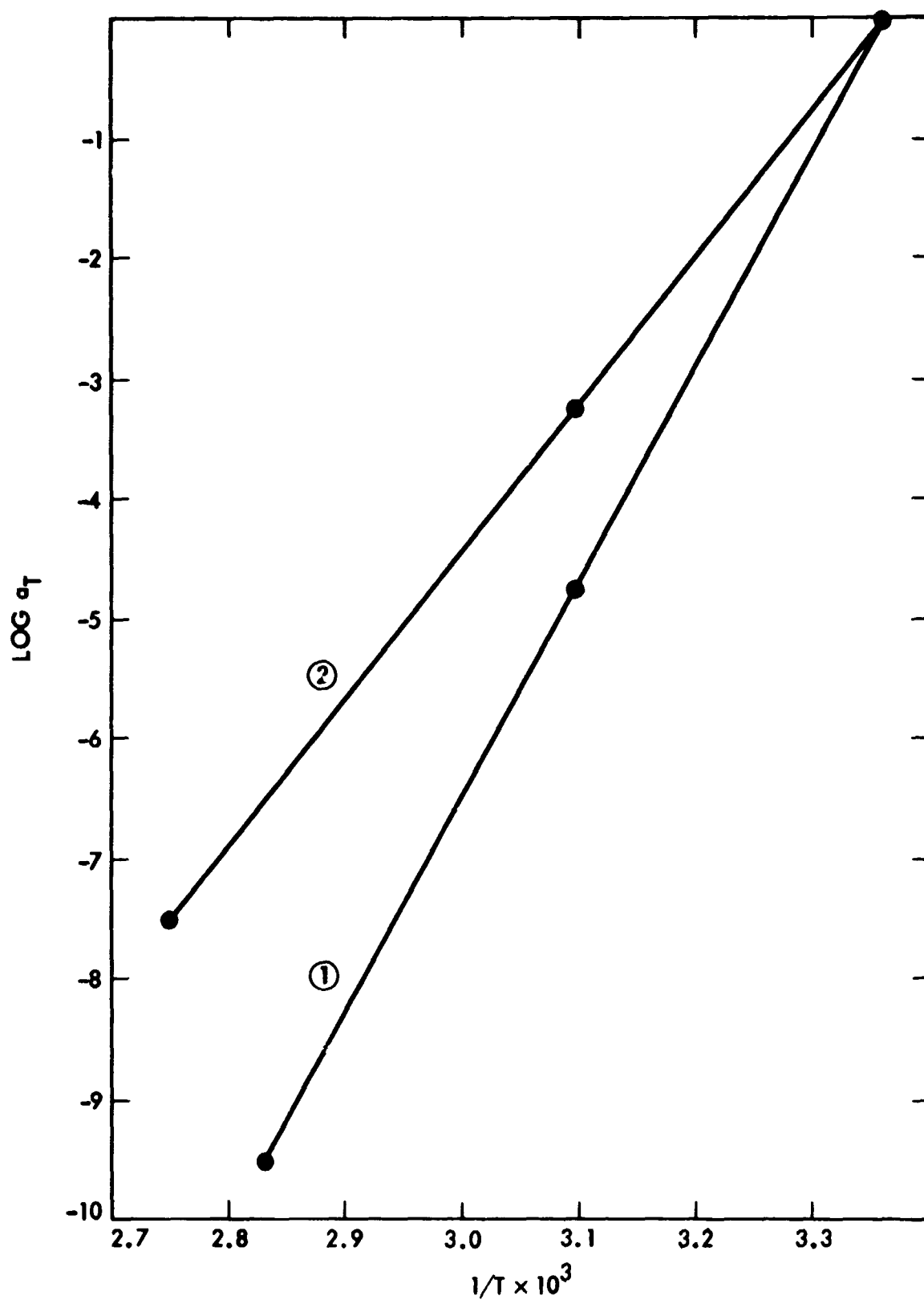Figure 33. Dependence of σ_b on t_b for FVMQ 3

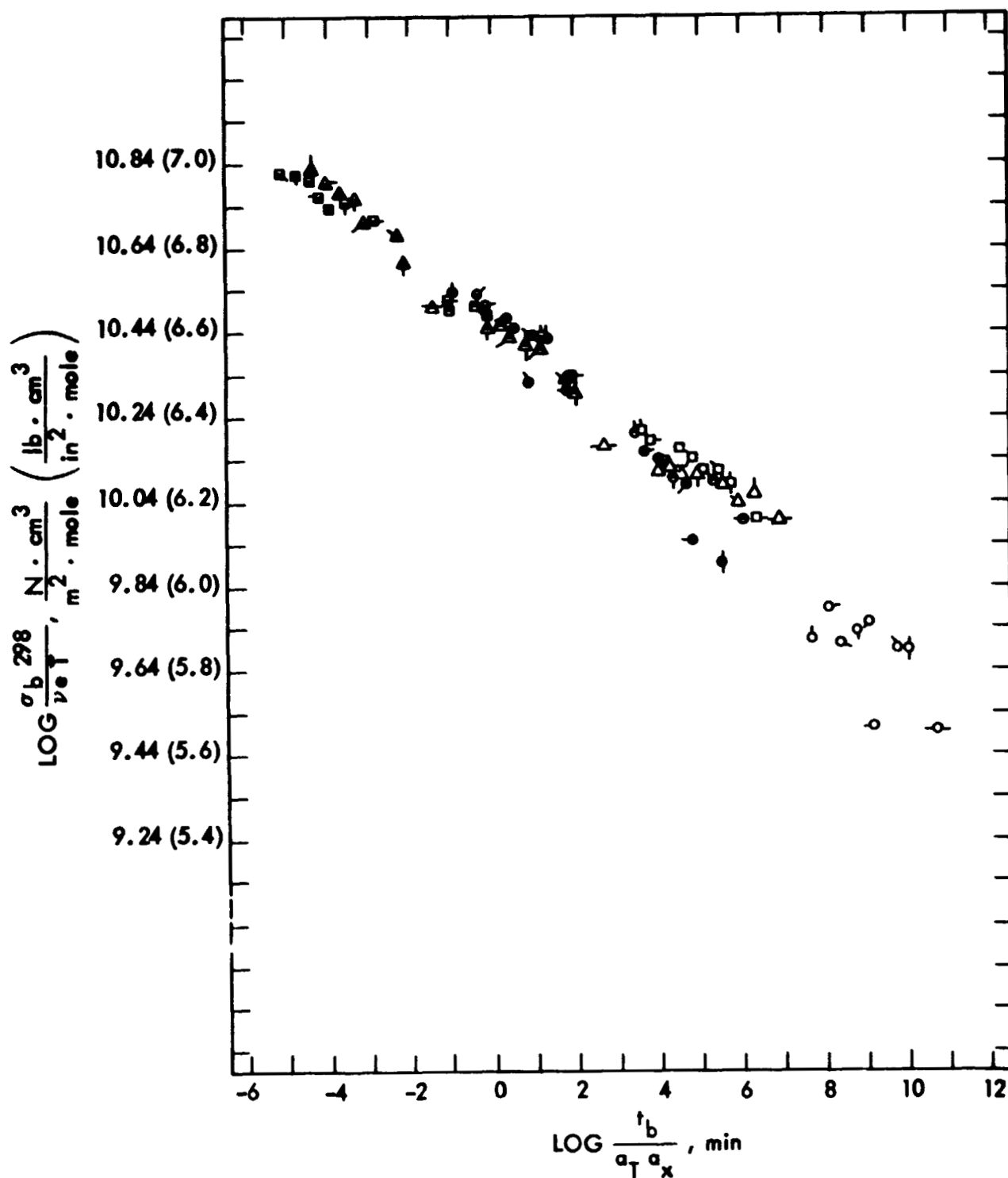Figure 34.   Temperature Dependence of a_T. ① NBR 2, ② FVMQ 3

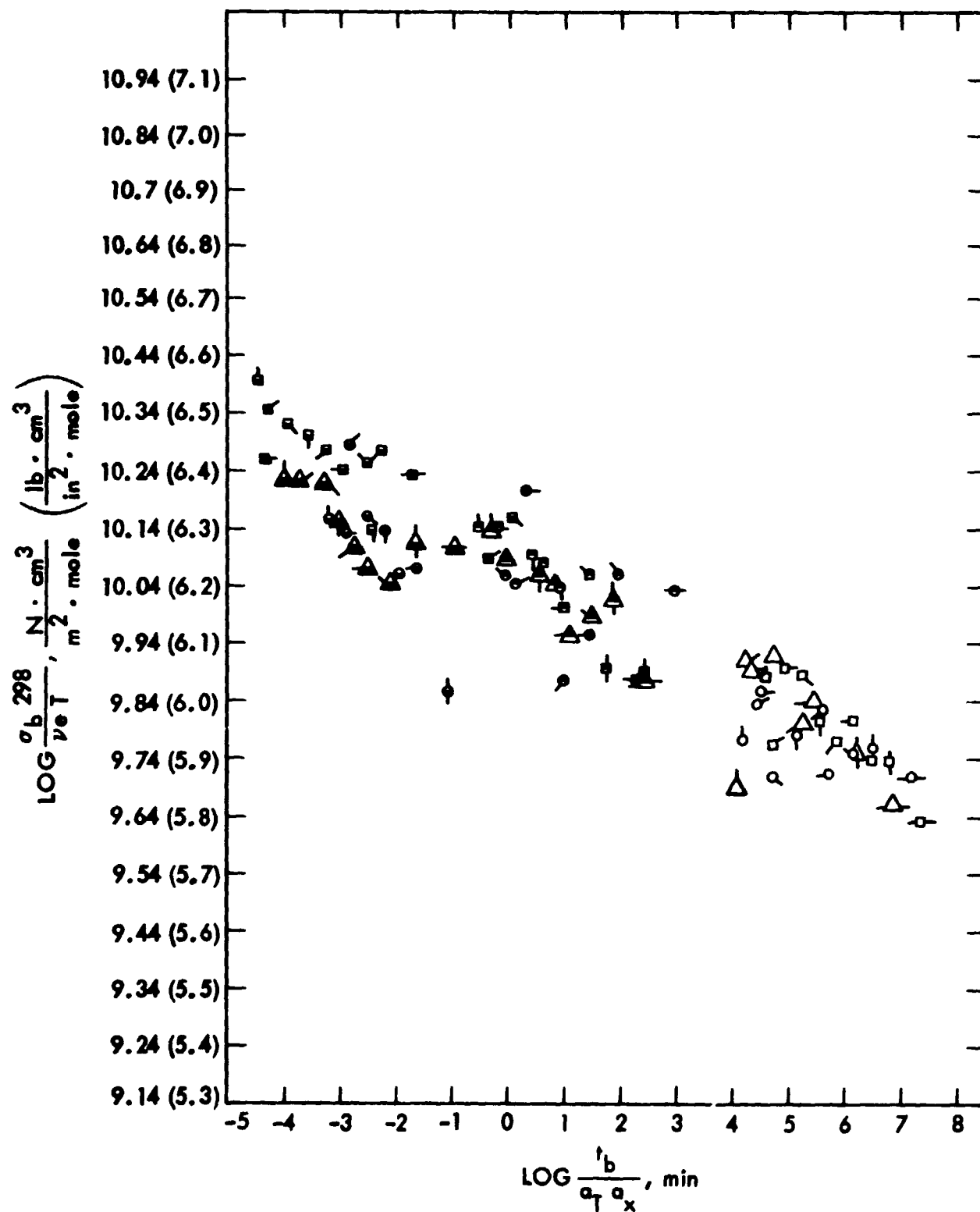Figure 35. Dependence of Reduced σ_b on Reduced t_b for NBR 2

Figure 36.   Dependence of Reduced Stress at Break to Reduced t_b for FVMQ 3

factor is log a_x as mentioned earlier. Figures 35 and 36 can thus be used to predict service life at long times when the cross-link density of the elastomer tested is known.

The effect of temperature on the time to break, t_b, of NBR 2 and FVMQ 3 at various stress values are shown in Figures 37 and 38, respectively. They were obtained from σ_b vs. log t curves using the slopes of the failure envelope plots of Figures 30-35. The curves in Figures 37 and 38, as well as Figures 35 and 36, represent the major results of measurements made for predicting the lifetime of these elastomers. It must be emphasized that values are time to break in absence of chemical degradation. Because of the scatter in the data, estimated t_b's can vary up to a hundred fold at a given stress level. The curves in Figures 35-38 show the minimum time required to break; that is, failure cannot occur sooner than the times indicated, but it could take much longer, up to about 100 times longer to fail. To estimate t_b, lines from the ordinate, representing stress levels, are drawn to the curves and then traced to the abscissa, the time axis. For example, at a stress level of 690 kP (100 psi), it can be found from Figure 38 that it should take FVMQ 3 32 minutes to break at 363 K (90°C), 69 days at 323 K (50°C) and > 1.92×10^5 years at 198 K (25°C). These numbers show the dramatic influence of temperature on t_b.

Similarly, at a stress level of 2760 kP (400 psi), it should take NBR 2 (Figure 37) 3.2 minutes to break at 353 K (80°C), 22 days at 323 K (50°C), and 3300 years at 298 K (25°.). The susceptibility of the mechanical properties of the elastomers to temperature are again shown by these values. An increase in temperature from 25 to 80°C is predicted to decrease the t_b of NBR by about 8 orders of magnitude.

The plots in Figures 35 and 36 are used to estimate t_b when the cross-link density, ν_e, and the two shift factors, a_T and a_x, are known. Thus, these curves are useful in estimating lifetimes in presence of chemical degradation, because changes in ν_e reflects chemical degradation. It is assumed in these calculations that the chemical degradation occurs before the sample is subjected to a mechanical load. The fol-
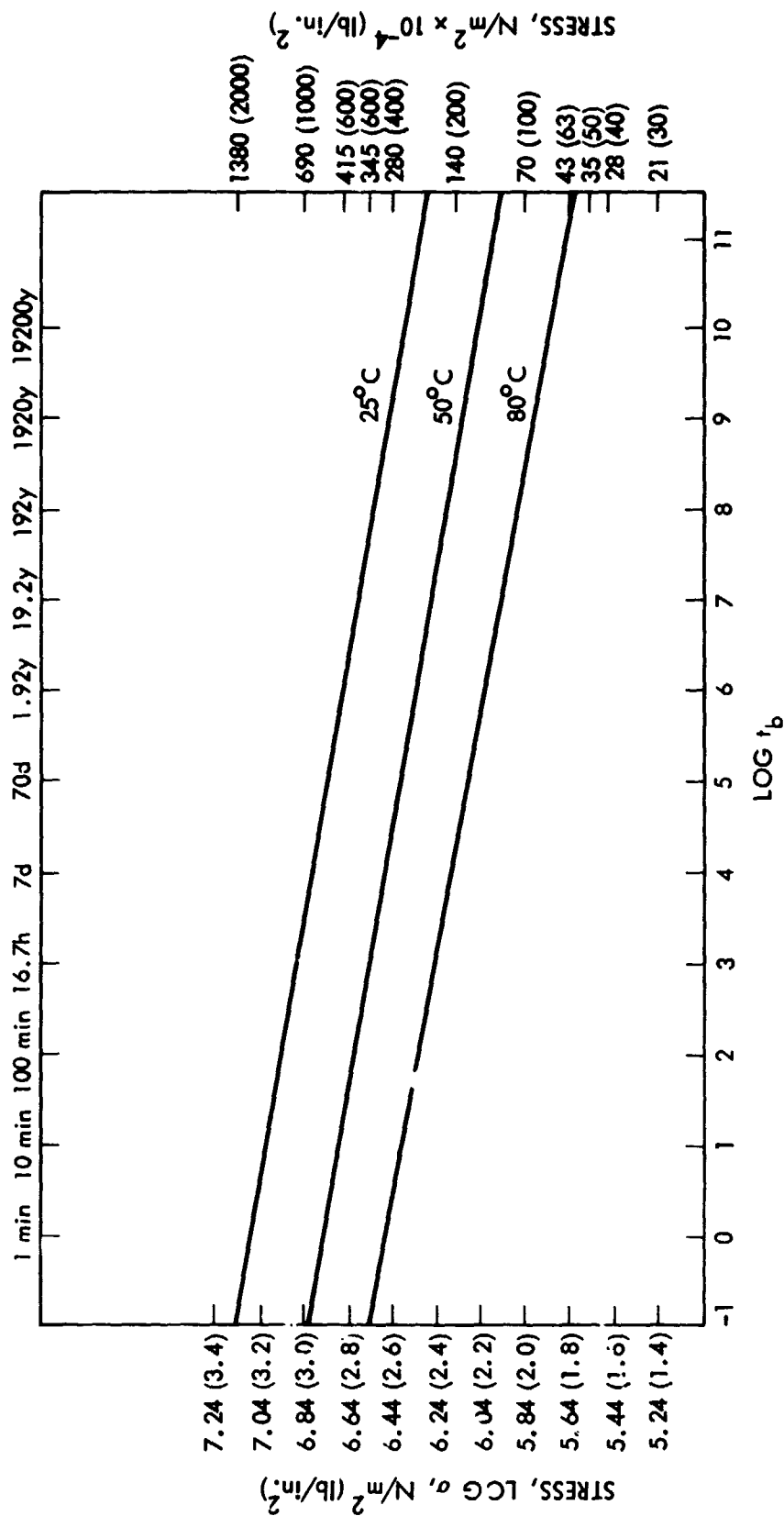
Figure 37. Tensile Stress Versus Time to Rupture as a Function of Temperature for NBR 2
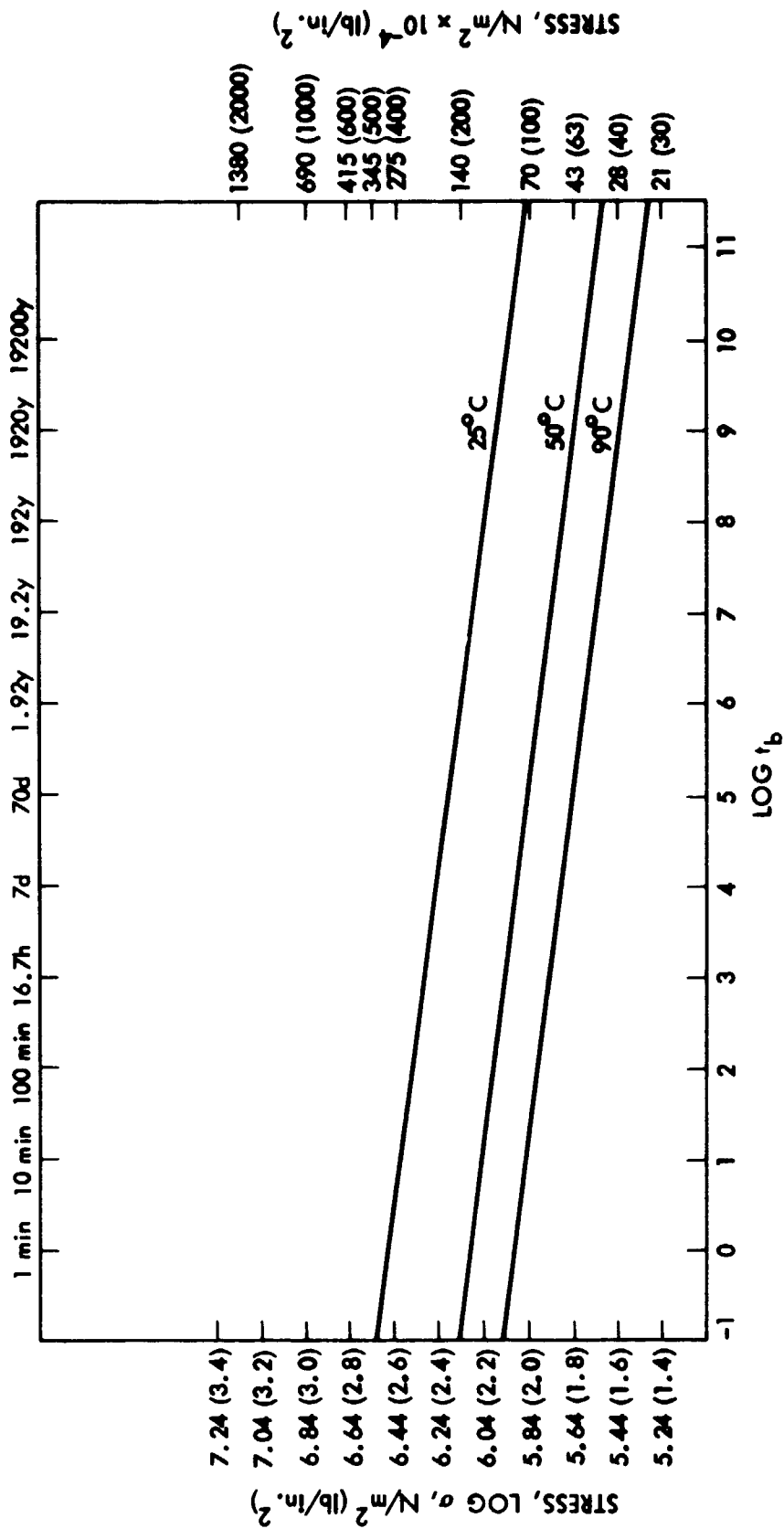
Figure 38.   Tensil Stress Versus Time to Rupture as a Function of Temperature for FVMQ 3

60

lowing examples are illustrative: at a stress level of 434 kP (63 psi) and at 363 K, a_T = 7.5 and a_X = 0. The ν_e of unaged FVMQ 3 is 240 moles/m^3 (240 x 10^{-6} moles/cm^3). The t_b is calculated as follows:

$$\log \sigma = 1.80$$
$$\log \nu_e = -3.619$$
$$\log (\sigma_b/\nu_e)(298/363) = 1.80 + 3.619 - 0.09 = 5.329$$
$$\log t_b/a_T a_X = 12.5 \text{ (from master curve, Figure 36)}$$
$$\log t_b = 12.5 - 7.5 + 0 = 5$$
$$t_b = 70 \text{ days}$$

The value of $t_b/a_T a_X$ was obtained by the linear extrapolation of the master curve (Figure 36). Previous work with other elastomers has shown that the curve is linear over very wide ranges in the time scale. (The same t_b value is obtained when it is estimated from Figure 38). After 240 hours of aging in Fuel III at 150°C, the ν_e of FVMQ 3 drops down to 140 moles/m^3 from 240. Under the same conditions of the above example, the t_b of the aged sealant is calculated to be 35.5 minutes!

These calculations demonstrate the marked effects of aging at high temperatures; however, in many cases these materials may not be subjected to such high thermal or mechanical stresses and could have very long lifetimes, especially FVMQ. For critical applications, new materials will be required.

SECTION IV.

SUMMARY

Data obtained from both chemical stress relaxation and tensile stress vs. time to break measurements on NBR, FVMQ and T based seal and sealant compositions were used to predict their lifetimes. Stress relaxation experiments could not be carried out with the polysulfide sealant T because of inherent difficulties and tensile testing was also limited to samples aged in fuels at lower temperatures. Treatment of the data from chemical stress relaxation measurements in

fuels yielded indicated lifetimes to a given extent of stress relaxation. Stress relaxations were measured over a relatively short period of time and, therefore, predictions to larger extent of relaxation could not be obtained. From stress and strain vs. time to break measurements at different temperatures, curves were constructed which were used to predict lifetime in the absence of chemical degradation. These curves, constructed from data obtained at only 3 temperatures, were not as complete as desired. The existence of a_χ, the cross-link density-time shift factor, and its incorporation into the time scale, make it possible to estimate the lifetimes in presence of chemical degradation, if it is assumed that the degradation and resultant change in v_e occur before the sample is subjected to stress.

Stress relaxation experiments furnished other information as well: the nature of network breakdown, whether scission or cross-linking, or both; the site of the breakdown, whether at the cross-links or at the backbone; the relative rates of degradation, etc. It was shown both by stress relaxation and sol-gel determinations that breakdown in both NBR and T, when aged in alternate fuels at elevated temperatures, occurs at the polymer backbone at random. Scission in FVMQ is at the cross-links. The faster relaxation of FVMQ in air than in the inert atmoshpere of nitrogen showed that bond cleavage is caused more by atmospheric oxygen than by thermal effects. Much severer degradation of the FVMQ was observed in liquid fuel heated in sealed containers than when exposed to fuel vapor at the same temperatures. This was explained on the grounds that ionic nature of the strong Si-O bonds, present in both the cross-links and the backbone chain, may make them susceptible to electrophilic and nucleophilic attack by possible acidic and basic impurities formed in the FVMQ and the fuel during thermal breakdown. In the liquid fuel environment, these impurities would be in contact with the FVMQ, whereas in the fuel vapor, they would be washed away from the reaction zone. Nor would it be expect d that any acidic or basic tars formed in the fuel volatilize enough to get into the vapor phase at the test temperatures.

It was shown that degradation of NBR and T in highly aromatic fuels is very fast as compared with that of FVMQ. The rate of relaxation is directly proportional to the aromatic hydrocarbon content of the fuel. Temperature has a dramatic effect on the time to break, t_b, of the rubbers tested, even in the absence of chemical degradation.

SECTION V

REFERENCES

1.   A. V. Tobolsky, "Properties and Structure of Polymers," p. 258, John Wiley and Sons, Inc., New York, 1960.

2.   A. V. Tobolsky, I. B. Prettyman, and J. H. Dillon, J. Appl. Phys., $\underline{15}$, 309, 1944.

3.   A. V. Tobolsky, "Properties and Structure of Polymers," p. 223, John Wiley and Sons, Inc., New York, 1960

4.   P. J. Flory and J. Rehner, Jr., J. Chem. Phys. $\underline{11}$, 521 (1943).

5.   L. Pauling, "The Nature of the Chemical Bond," Cornell University Press, Ithaca, N.Y., 3rd Ed., 1960.

6.   W. Noll, "Chemistry and Technology of Silicones," Academic Press, New York, 1968. p. 147.

7.   N. B. Hannay and C. P. Smyth, J. Am. Chem. Soc. $\underline{68}$, 171 (1946).

8.   L. Pauling, J. Phys. Chem. $\underline{56}$, 361, 1952.

9.   M. M. Horikx, J. Poly. Sci., $\underline{19}$, 445, 1956.

10.   R. F. Landel and R. F. Fedors, "Fracture Processes in Polymeric Solids," pp. 361-458, B. Rosen Editor, Interscience Publishers, New York, 1964.